NASA Reference Publication 1073

Comparisons Between Nimbus 6 Satellite and Rawinsonde Soundings for Several Geographical Areas

Nine-Min Cheng and James R. Scoggins

JANUARY 1981

NASA

NASA Reference Publication 1073

Comparisons Between Nimbus 6 Satellite and Rawinsonde Soundings for Several Geographical Areas

Nine-Min Cheng and James R. Scoggins
Texas A&M University
College Station, Texas

National Aeronautics
and Space Administration

**Scientific and Technical
Information Branch**

1981

ACKNOWLEDGMENTS

The authors thank Dr. Vance Moyer, Dr. Oliver Aberth, and Dr. Kenneth Brundidge for their comments and recommendations regarding the scientific content of this report, Miss Doreen Westwood and Mr. Jsun-Chein Cheng for drafting the figures, and Mrs. Karen Hood for typing the final manuscript.

The research was supported by the U. S. Army Research Office, Research Triangle Park, North Carolina, under Grant DAAG 29-76-G-0078 to the Department of Meteorology, Texas A&M University.

This report is published with the permission of the U. S. Army Research Office for use in connection with studies utilizing space technology for weather-related programs in progress in the Atmospheric Sciences Division, Space Sciences Laboratory, NASA, Marshall Space Flight Center.

TABLE OF CONTENTS

		Page
ACKNOWLEDGEMENTS		ii
TABLE OF CONTENTS		iii
LIST OF FIGURES		v
LIST OF TABLES		ix
1.	INTRODUCTION	1
2.	BACKGROUND TO RESEARCH	2
3.	DATA	4
	a. Satellite	4
	b. Rawinsonde	4
4.	AREAS ANALYZED AND SYNOPTIC CONDITIONS	7
	a. Areas	7
	b. Synoptic conditions	7
5.	METHODS OF DATA ANALYSIS	11
	a. Pairing of profiles	11
	b. Parameters considered	14
	1) Temperature and dew-point temperature	14
	2) Mixing ratio	15
	3) Thickness	15
	4) Lapse rate of temperature	15
	5) Precipitable water	16
	6) Stability indexes	16
	c. Stratification of data	16

TABLE OF CONTENTS (Continued)

Page

d. Computation of statistical parameters and distributions 17

6. RESULTS 18

a. Temperature 18

b. Dew-point temperature 35

c. Thickness 36

d. Mixing ratio 42

e. Precipitable water 48

f. Stability 48

1) Lapse rate 49

2) Showalter Index 49

3) Vertical Totals Index 52

7. SUMMARY AND CONCLUSIONS 57

a. Summary 57

b. Conclusions 57

REFERENCES 59

APPENDIX A 61

APPENDIX B 63

LIST OF FIGURES

Figure		Page
1	Satellite sounding locations (crosses) along Nimbus 6 orbit between 1710 and 1727 GMT on 25 August 1975, and rawinsonde stations (dots) for the area covered by the satellite data	5
2	Satellite sounding locations (crosses) along Nimbus 6 orbit between 0735 and 0740 GMT on 3 September 1975, and rawinsonde stations (dots) for the area covered by the satellite data	6
3	The four geographical areas considered in this study (Area I - central United States; Area II - Caribbean Sea; Area III - central Canada; and Area IV - western United States)	8
4	Surface map covering Areas I, II and III at 1800 GMT on 25 August 1975 (contours in millibars with first one or two digits omitted)	9
5	Surface map covering Area IV at 0600 GMT on 3 September 1975 (contours in millibars with first two digits omitted)	10
6	Pairings of satellite sounding locations (solid dots) and rawinsonde stations (open circles) for Area I	12
7	Pairings of satellite sounding locations (solid dots) and rawinsonde stations (open circles) for Area II	12
8	Pairings of satellite sounding locations (solid dots) and rawinsonde stations (open circles) for Area III	13
9	Pairings of satellite sounding locations (solid dots) and rawinsonde stations (open circles) for Area IV	13
10	Smoothed contours of average surface terrain height (m) for the western United States encompassing Area IV	21
11	Examples of the (a) "closest" and (b) "poorest" agreement between paired profiles for Area I (From Moyer, et al., 1978)	22

LIST OF FIGURES (Continued)

Figure		Page
12	Examples of the (a) "closest" and (b) "poorest" agreement between paired profiles for Area II	23
13	Examples of the (a) "closest" and (b) "poorest" agreement between paired profiles for Area III	24
14	Examples of the (a) "closest" and (b) "poorest" agreement between paired profiles for Area IV	25
15	Temperature discrepancies between satellite and rawinsonde data as a function of pressure for selected stations in each of the four geographical areas	30
16	Cumulative frequency distributions of discrepancies in temperature in the layers surface to 500 mb, 500 to 300 mb, and 300 to 100 mb for Area I (central United States)	33
17	Cumulative frequency distributions of discrepancies in temperature in the layers surface to 500 mb, 500 to 300 mb, and 300 to 100 mb for Area II (Caribbean) . .	33
18	Cumulative frequency distributions of discrepancies in temperature in the layers surface to 500 mb, 500 to 300 mb, and 300 to 100 mb for Area III (Canada) . .	34
19	Cumulative frequency distributions of discrepancies in temperature in the layers surface to 500 mb, 500 to 300 mb, and 300 to 100 mb for Area IV (western United States)	34
20	Cumulative frequency distributions of discrepancies in dew-point temperature in the layers surface to 500 mb, and 500 to 300 mb for Area I (central United States)	37
21	Cumulative frequency distributions of discrepancies in dew-point temperature in the layers surface to 500 mb, and 500 to 300 mb for Area II (Caribbean)	37
22	Cumulative frequency distributions of discrepancies in dew-point temperature in the layers surface to 500 mb, and 500 to 300 mb for Area III (Canada)	38

LIST OF FIGURES (Continued)

Figure		Page
23	Cumulative frequency distributions of discrepancies in dew-point temperature in the layers surface to 500 mb, and 500 to 300 mb for Area IV (western United States)	38
24	Cumulative probability frequency distributions of normalized thickness discrepancies within the layers surface to 500 mb, 500 to 300 mb, and 300 to 100 mb for the central United States (Area I)	43
25	Cumulative probability frequency distributions of normalized thickness discrepanceis within the layers surface to 500 mb, 500 to 300 mb, and 300 to 100 mb for the Caribbean (Area II)	43
26	Cumulative probability frequency distributions of normalized thickness discrepancies within the layers surface to 500 mb, 500 to 300 mb, and 300 to 100 mb for Canada (Area III)	44
27	Cumulative probability frequency distributions of normalized thickness discrepancies within the layers surface to 500 mb, 500 to 300 mb, and 300 to 100 mb for the western United States (Area IV)	44
28	Cumulative frequency distributions of discrepancies in mixing ratio in the layers surface to 500 mb and 500 to 300 mb for the central United States	46
29	Cumulative frequency distributions of discrepancies in mixing ratio in the layers surface to 500 mb and 500 to 300 mb for the Caribbean	46
30	Cumulative frequency distributions of discrepancies in mixing ratio in the layers surface to 500 mb and 500 to 300 mb for Canada	47
31	Cumulative frequency distributions of discrepancies in mixing ratio in the layers surface to 500 mb and 500 to 300 mb for the western United States	47
32	Cumulative frequency distributions of discrepancies in the lapse rate of temperature within the layers surface to 500 mb, 500 to 300 mb, and 300 to 100 mb for Area I (central United States)	50

LIST OF FIGURES (Continued)

Figure		Page
33	Cumulative frequency distributions of discrepancies in the lapse rate of temperature within the layers surface to 500 mb, 500 to 300 mb, and 300 to 100 mb for Area II (Caribbean)	50
34	Cumulative frequency distributions of discrepancies in the lapse rate of temperature within the layers surface to 500 mb, 500 to 300 mb, and 300 to 100 mb for Area III (Canada)	51
35	Cumulative frequency distributions of discrepancies in the lapse rate of temperature within the layers surface to 500 mb, 500 to 300 mb, and 300 to 100 mb for Area IV (western United States)	51

LIST OF TABLES

Table		Page
1	Maximum, minimum, and mean distance (km) between paired satellite sounding locations and rawinsonde stations for Areas I, II, III and IV	11
2	Selected statistics of temperature discrepancies between Nimbus 6 satellite and weighted rawinsonde data for all four areas (°C)	19
3	Maximum absolute discrepancy between Nimbus 6 and rawinsonde temperatures for each profile pair for Area I (°C)	26
4	Maximum absolute discrepancy between Nimbus 6 and rawinsonde temperatures for each profile pair for Area II (°C)	27
5	Maximum absolute discrepancy between Nimbus 6 and rawinsonde temperatures for each profile pair for Area III (°C)	27
6	Maximum absolute discrepancy between Nimbus 6 and rawinsonde temperatures for each profile pair for Area IV (°C)	28
7	Mean and standard deviation of temperature discrepancies (°C) between Nimbus 6 satellite and weighted rawinsonde data stratified by three layers: (A) Surface to 500 mb; (B) 500 to 300 mb; (C) 300 to 100 mb	32
8	Means and standard deviations of discrepancies and the root-mean-square of discrepancies between satellite and weighted rawinsonde dew-point temperatures for Areas I, II, III and IV (°C)	35
9	Means and standard deviations of discrepancies in dew-point temperature within the layers surface to 500 mb, and 500 to 300 mb for all four areas (°C)	36
10	Means and standard deviations of thickness discrepancies determined from thicknesses computed from mean temperature and mean virtual temperature for all four areas (m)	40
11	Means and standard deviations of discrepancies between (a) Nimbus 5 satellite and rawinsonde and (b) Nimbus 6 satellite and rawinsonde layer thicknesses (m)	41

LIST OF TABLES (Continued)

Table		Page
12	Means and standard deviations of normalized discrepancies in thickness for the layers surface to 500 mb, 500 to 300 mb, and 300 to 100 mb for all areas (m)	42
13	Means and standard deviations of discrepancies (g kg^{-1}) between Nimbus 6 satellite and weighted rawinsonde mixing ratio data stratified into two layers: (A) surface to 500 mb, and (B) 500 to 300 mb	45
14	Means and standard deviations of discrepancies (cm) between Nimbus 6 satellite and weighted rawinsonde precipitable water for all four areas	48
15	Means and standard deviations of discrepancies ($°C\ km^{-1}$) between Nimbus 6 satellite and weighted rawinsonde lapse rate data stratified into three layers: (A) surface to 500 mb; (B) 500 to 300 mb; and (C) 300 to 100 mb	49
16	Discrepancies in the Showalter Index derived from satellite and rawinsonde data for Area I (central United States)	53
17	Same as Table 16, but for Area II (Caribbean)	53
18	Same as Table 16, but for Area III (Canada)	54
19	Same as Table 16, but for Area IV (western United States)	54
20	Discrepancies in the Vertical Totals Index derived from satellite and rawinsonde data for Area I (central United States)	55
21	Same as Table 20, but for Area II (Caribbean)	55
22	Same as Table 20, but for Area III (Canada)	56
23	Same as Table 20, but for Area IV (western United States)	56

COMPARISONS BETWEEN NIMBUS 6 SATELLITE AND RAWINSONDE SOUNDINGS FOR SEVERAL GEOGRAPHICAL AREAS*

Nine-Min Cheng and James R. Scoggins
Department of Meteorology
Texas A&M University

1. INTRODUCTION

Great strides have been made within the past decade toward the measurement of atmospheric vertical profiles of temperature and moisture from satellite radiation data. The high resolution infrared radiometers carried by the Nimbus 3, 4, 5, and 6 satellites provided valuable radiation data from which the three-dimensional structure of the atmosphere could be determined or inferred. In addition, Nimbus 5 and 6 carried microwave sensors from which vertical profiles of temperature and moisture have been determined even in the presence of various cloud conditions.

The objective of this research is to examine the differences between rawinsonde and Nimbus 6 satellite sounding data for several geographical areas, and to determine the accuracy of the satellite data relative to rawinsonde data. The following parameters are considered: temperature, dew-point temperature, mixing ratio, thickness, lapse rate of temperature, precipitable water, and stability. Relative "errors" in satellite data will be presented as a function of geographic area, synoptic conditions, and surface characteristics.

---

* Research supported by U. S. Army Research Office, Research Triangle Park, North Carolina, under Grant DAAG 29-76-0078 to the Department of Meteorology, Texas A&M University.

2. BACKGROUND TO RESEARCH

An objective of meteorological satellite technology has been to measure remotely key atmospheric parameters that would permit a description of the atmosphere in quantitative terms. The most desirable atmospheric parameters to observe from satellites are those that are utilized in the basic hydrodynamic and thermodynamic equations that apply to the atmosphere. Some of the major parameters are pressure, temperature, moisture, and wind (Shenk and Salomonson, 1970).

The first vertical profiles of both temperature and water vapor were determined from measurements of two infrared spectrometers carried by the Nimbus 3 satellite. These data provided the first analysis of the three-dimensional thermodynamic structure of the atmosphere from satellite observations. The first studies (Wark and Hilleary, 1969; Hanel and Conrath, 1969) compared individual satellite temperature profiles with corresponding rawinsonde profiles; relatively good agreement was found.

The Nimbus 5 satellite carried a microwave spectrometer (NEMS) (Staelin et al., 1972) that provided temperature and moisture profiles even in the presence of clouds. An investigation of temperature profiles determined from the NEMS indicated a root-mean-square (RMS) discrepancy between NEMS and rawinsonde data between 2.5 and 4 K (Waters et al., 1975). Discrepancies ranging between 1 and 4 K over an altitude range of 1 to 20 km were found, with the largest discrepancies occurring near the tropopause and near the surface (Staelin et al., 1973). Another study (Smith et al., 1975) showed that, in the troposphere, the discrepancies between satellite and rawinsonde soundings were generally small except in the tropopause region between 300 and 100 mb. These large differences resulted from vertical resolution limitations of the satellite sensor. The same study indicated that significantly better profile results could be achieved from the combined data of infrared and microwave measurements than could be achieved by either used individually. A case study

(Horn et al., 1975) was made comparing the Nimbus 5 satellite sounding temperatures obtained at 1700 GMT with those obtained from radiosonde at 1200 GMT and 0000 GMT. Since the synoptic pattern changed quite rapidly between 1200 GMT and 0000 GMT in this case, the sign of the difference between satellite and rawinsonde temperatures changed for 1700 GMT Nimbus minus 1200 GMT radiosonde, and for 1700 GMT Nimbus minus 0000 GMT radiosonde.

Satellite-derived thicknesses were compared with rawinsonde layer thicknesses by Wilcox and Sanders (1976). Standard deviations of 45, 49, and 115 m for the layers 1000-500, 500-250 and 250-50 mb, respectively, were found.

Estimates of water vapor (mixing ratio) determined from satellite data contain errors which often exceed 30% of the values measured by nearby radiosondes (Weinreb, 1977). However, satellite-derived precipitable water was found to be within 0.5 cm RMS with the horizontal distribution represented quite well (Hillger and Von der Haar, 1977).

The Nimbus 6 satellite carries improved instruments for sensing the temperature sounding. In this research, satellite sounding data determined from infrared and microwave radiation data from the Nimbus 6 satellite will be compared with the weighted (linearly interpolated) rawinsonde data.

3. DATA

a. Satellite

Profiles of temperature and moisture determined from Nimbus 6 satellite radiation data (Smith et al., 1975; Staelin et al., 1975) provided by the National Environment Satellite Service are used in this research. The data were obtained along two different satellite paths. Figure 1 shows the satellite sounding locations (crosses) along the orbit from the Caribbean to Canada between 1710 and 1727 GMT on 25 August 1975, and the rawinsonde stations (dots) for the same area. Figure 2 shows the satellite (crosses) and rawinsonde (dots) sounding locations along the orbit over the western United States (from north to south) between 0735 and 0740 GMT on 3 September 1975. Temperature and dew-point temperature data are provided for 21 levels for each sounding at 1000, 950, 920, 850, 780, 700, 670, 620, 570, 500, 475, 430, 400, 350, 300, 250, 200, 150, 135, 115, and 100 mb.

b. Rawinsonde

Rawinsonde data were requested from the National Climatic Center, Asheville, North Carolina, for the two areas covered by the satellite data mentioned above. These data were requested for 1200 GMT on 25 August 1975, 0000 GMT on 26 August 1975, and 0000 GMT and 1200 GMT on 3 September 1975. In order to obtain rawinsonde data corresponding to the 21 levels in the satellite sounding data, each rawinsonde sounding was plotted on a Skew T-log p chart, and temperature and dew-point temperature interpolated to the level as required.

Fig. 1. Satellite sounding locations (crosses) along Nimbus 6 orbit between 1710 and 1727 GMT on 25 August 1975, and rawinsonde stations (dots) for the area covered by the satellite data.

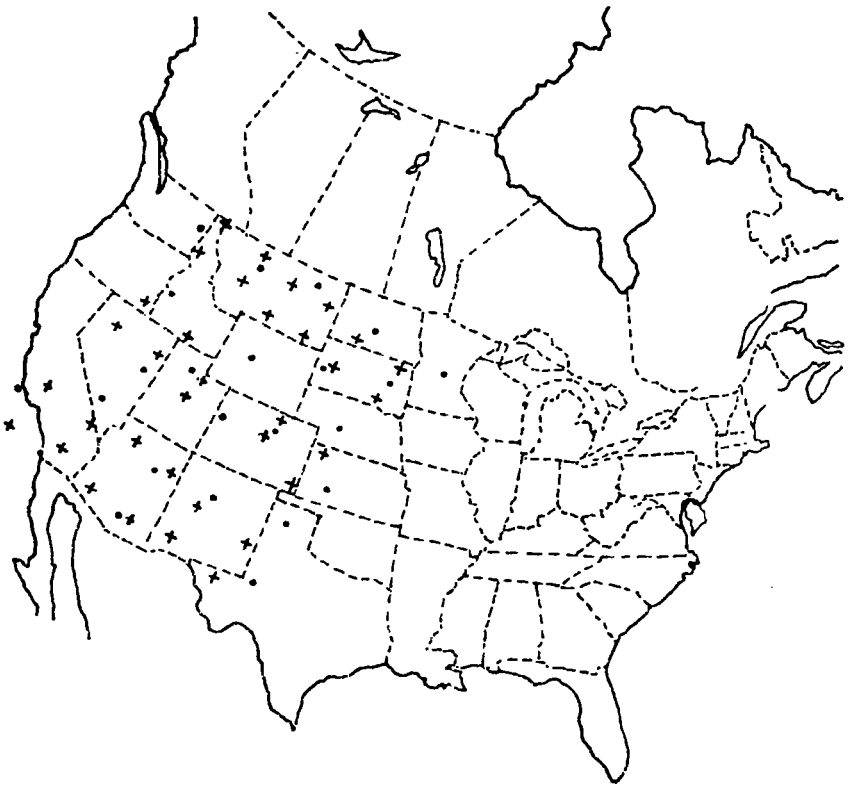

Fig. 2. Satellite sounding locations (crosses) along Nimbus 6 orbit between 0735 and 0740 GMT on 3 September 1975, and rawinsonde stations (dots) for the area covered by the satellite data.

4. AREAS ANALYZED AND SYNOPTIC CONDITIONS

a. Areas

Satellite and rawinsonde sounding data were obtained for four geographical areas in order to compare the soundings for different surface and synoptic conditions. Figure 3 shows the four areas which are: (1) central United States - Area I; (2) Caribbean Sea - Area II; (3) central Canada - Area III; and (4) western United States - Area IV. Areas I, II, and III are along the satellite orbit on 25 August 1975, while Area IV is along the satellite orbit on 3 September 1975. These four areas represent a variety of surface conditions including flat land, water, cold surface, and mountains, respectively.

b. Synoptic conditions

The surface map at 1800 GMT on 25 August 1975 is shown in Fig. 4. A cold front extends from the Hudson Bay southwestward through the central United States. The occluded part of the cold front associated with a deep cyclone was located in the eastern part of Area III. The mean surface temperature over Area III was about 12°C. The polar air was separated from the tropical air by the cold front extending through Area I, while Area II was covered entirely by an mT air mass.

Figure 5 shows the surface map in the vicinity of Area IV at 0600 GMT on 3 September 1975. The area was covered by a modified mP or cP air mass which was dry. No significant weather was occurring in Area IV although some clouds were present.

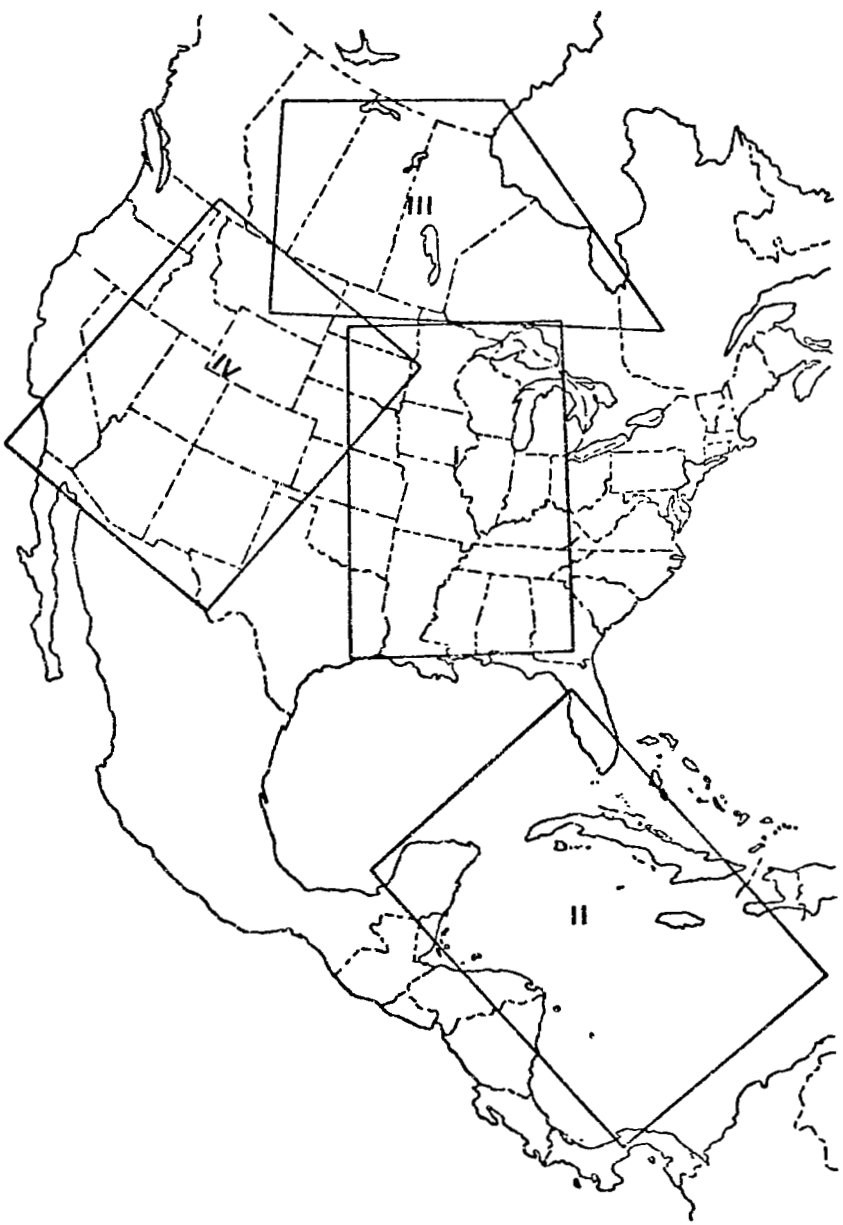

Fig. 3. The four geographical areas considered in this study (Area I - central United States; Area II - Caribbean Sea; Area III - central Canada; and Area IV - western United States).

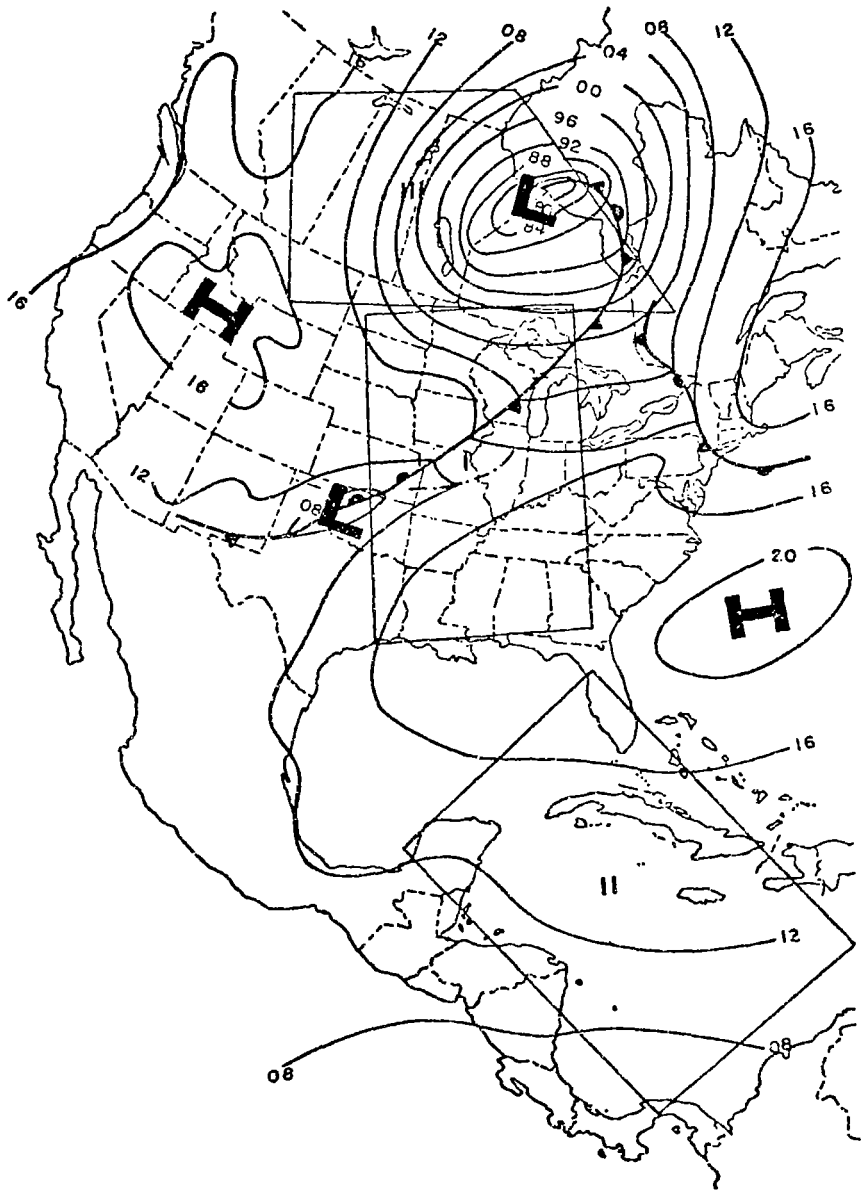

Fig. 4. Surface map covering Areas I, II, and III at 1800 GMT on 25 August 1975 (contours in millibars with first one or two digits omitted).

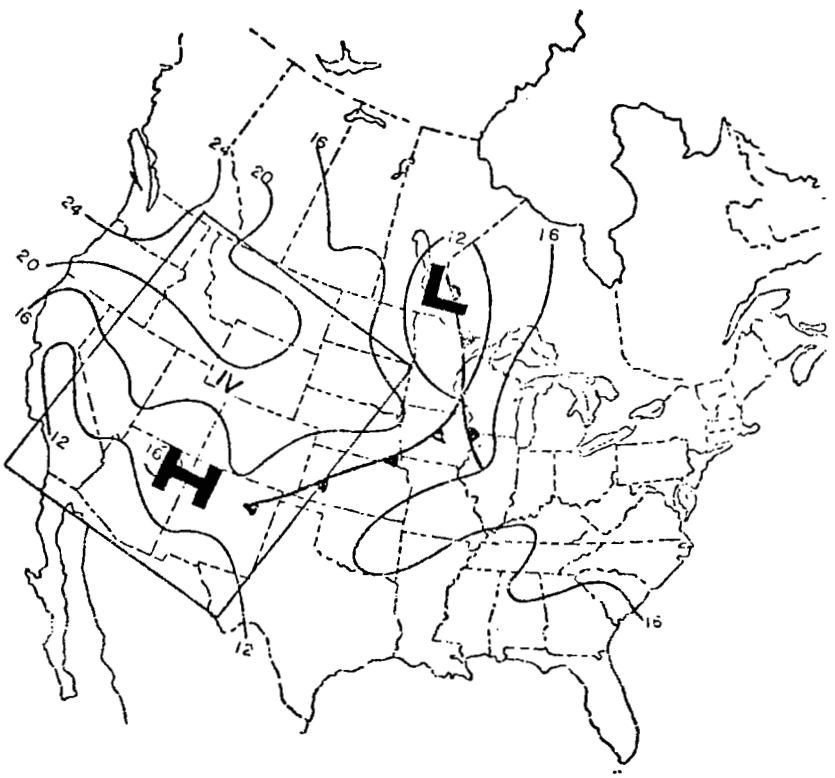

Fig. 5. Surface map covering Area IV at 0600 GMT on 3 September 1975 (contours in millibars with first two digits omitted).

5. METHODS OF DATA ANALYSIS

a. Pairing of profiles

For the purpose of comparison, satellite soundings were paired with the closest rawinsonde soundings. Since there were more satellite than rawinsonde soundings, not all available satellite data were used. Figures 6 through 9 show the pairings of satellite sounding locations (solid dots) and rawinsonde stations (open circles). There are 21, 9, 7, and 23 pairs for Areas I, II, III, and IV, respectively. Rawinsonde station numbers[1] are used to identify each pair of soundings in each area.

The Nimbus 6 satellite sensors scan from side to side along the suborbital path from an altitude of about 1100 km. The processing of the satellite data was such that spatial differences between satellite and rawinsonde soundings resulted. Table 1 shows the maximum, minimum, and mean distance[2] between paired satellite points and rawinsonde stations for each of the four areas.

Table 1. Maximum, minimum, and mean distance (km) between paired satellite sounding locations and rawinsonde stations for Areas I, II, III, and IV. Rawinsonde station numbers are enclosed in parentheses.

	Area I	Area II	Area III	Area IV
Maximum	246.9 (429)	432.0 (367)	407.4 (836)	308.6 (576)
Minimum	24.7 (451)	111.1 (001)	222.2 (119)	24.7 (274)
Mean	122.5	177.6	252.2	145.4
No. of pairs	21	9	7	23

Mean of all pairs for the four areas: 154.7 km

[1]Station names are given in Appendix A.
[2]Distance between each pair of soundings is given in Appendix B.

Fig. 6. Pairings of satellite sounding locations (solid dots) and rawinsonde stations (open circles) for Area I.

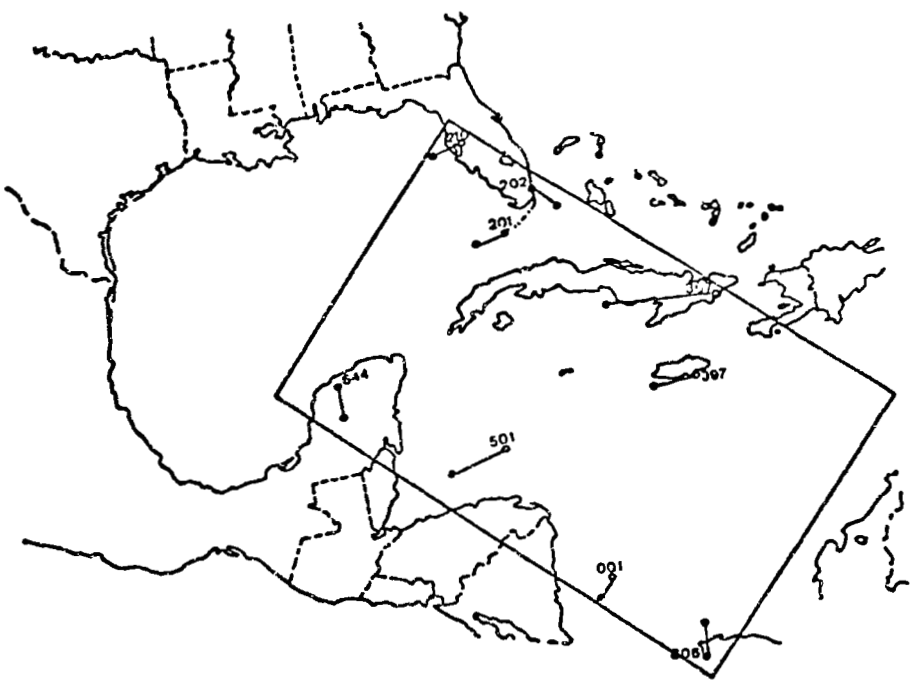

Fig. 7. Pairings of satellite sounding locations (solid dots) and rawinsonde stations (open circles) for Area II.

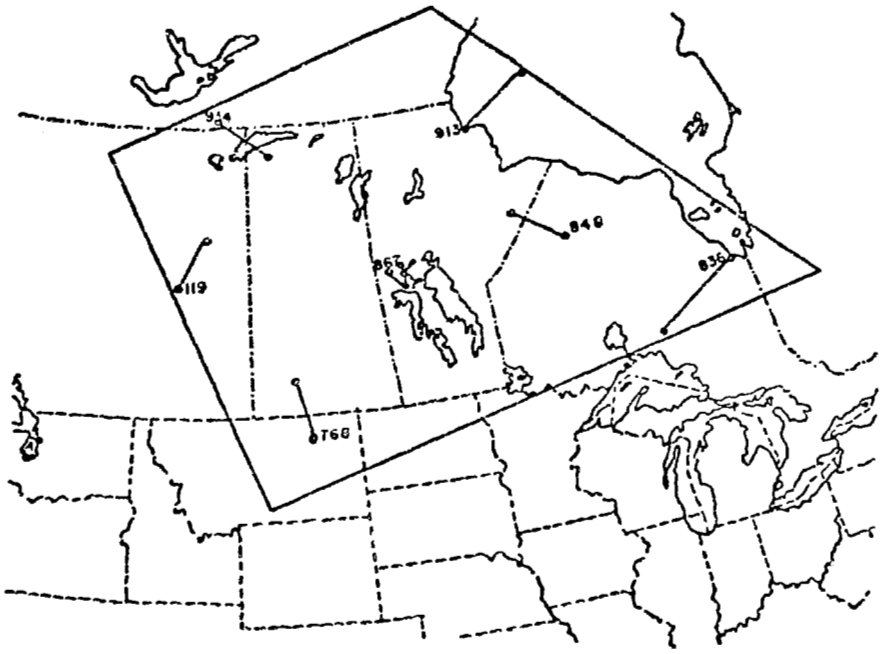

Fig. 8. Pairings of satellite sounding locations (solid dots) and rawinsonde stations (open circles) for Area III.

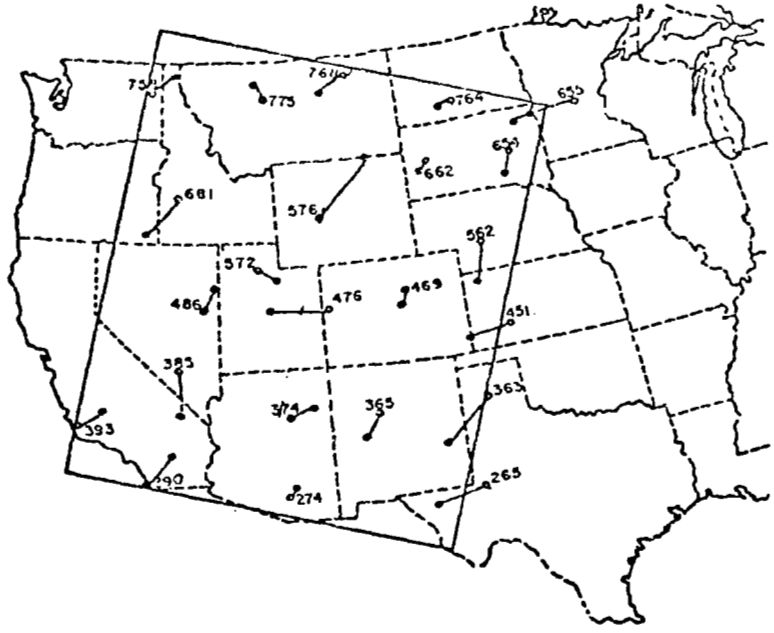

Fig. 9. Pairings of satellite sounding locations (solid dots) and rawinsonde stations (open circles) for Area IV.

The smallest mean difference was 122.5 km (Area I) and the largest mean difference was 252.2 km (Area III). The minimum distance between any pair of stations was 24.7 km (Areas I and IV), and the maximum was 432.0 km (Area II). The mean of all pairs over the four areas was 154.7 km which approximates 1.4° latitude. Part of the discrepancies between satellite and rawinsonde data can be accounted for by the distances between the sounding locations.

b. Parameters considered

Seven parameters were considered in this study for both satellite and rawinsonde data for each of the four areas. They are temperature, dew-point temperature, mixing ratio, thickness, lapse rate of temperature, precipitable water, and stability. The analysis procedure for each parameter is discussed below.

1) Temperature and dew-point temperature

For the purpose of comparing satellite and rawinsonde data, and in order to reduce the temporal difference to a minimum, the weighted means were taken of the 0000 and 1200 GMT rawinsonde soundings to approximate the sounding at the time of the satellite sounding. The weighted means for the satellite path on 25 August 1975 were computed by use of the equation

$$\bar{R} = (7/12)R_{1200} + (5/12)R_{0000}$$

where $\bar{R}$ is a weighted mean of the rawinsonde observations, R_{1200} and R_{0000} refer to the rawinsonde data at 1200 GMT on 25 August 1975 and 0000 GMT on 26 August 1975, respectively, and weights of 7/12 and 5/12 are used because the satellite sounding time is about 5 h after the 1200 GMT and 7 h before the 0000 GMT standard rawinsonde observations. For the satellite path on 3 September 1975, the weighted means were computed by use of the equation

$$\bar{R} = (4.5/12)R_{0000} + (7.5/12)R_{1200}.$$

The weights are different because the satellite sounding time was about 7½ h after the 0000 GMT, and 4½ h before the 1200 GMT standard rawinsonde observations. This weighting is equivalent to linear interpolation.

Each weighted rawinsonde sounding was plotted on a Skew T-log p chart, and temperature and dew-point temperature data corresponding to the 21 levels contained in the satellite soundings extracted and keypunched for computer processing.

2) Mixing ratio

Mixing ratio values for both satellite and rawinsonde soundings were obtained from soundings plotted on Skew T-log p diagrams. Values were read directly from the diagram at each of the 21 pressure levels for each satellite sounding. This was done by interpolating for the mixing ratio corresponding to the dew-point temperature. Also, the average mixing ratio for each layer defined by the sounding points was obtained by the equal-area method. Both sets of data were keypunched for computer processing.

3) Thickness

Satellite and weighted rawinsonde soundings were used to derive layer thicknesses. The thickness, ΔZ, of a layer between two isobaric surfaces is given by

$$\Delta Z = \frac{R\overline{T^*}}{g} \ln(p_1/p_2)$$

where R is the gas constant for dry air, $\overline{T^*}$ is the mean virtual temperature of the layer between pressures p_1 and p_2, and g is the acceleration due to gravity.

Here $\overline{T^*}$ is given by

$$\overline{T^*} = \overline{T} + \Delta T_m$$

where $\overline{T} = \frac{T_1 + T_2}{2}$,

$\Delta T_m = \overline{w}/6$,

$\overline{w}$ is the mean mixing ratio in the layer, and

T_1 and T_2 are the temperatures at p_1 and p_2, respectively.

4) Lapse rate of temperature

In this study, the lapse rate of temperature, γ, defined at a level (denoted by subscript 2) is given by

$$\gamma_2 = \frac{T_3 - T_1}{Z_3 - Z_1}$$

where the subscripts refer to successive pressure levels, T is

temperature, and Z is geopotential height.

5) Precipitable water

The precipitable water, W, was computed by use of the equation

$$W = \frac{1}{g} \int_{p_2}^{p_1} \overline{w} \, dp$$

where $\overline{w}$ is the mean mixing ratio for each layer between isobaric surfaces p_1 and p_2, and g is gravity.

6) Stability indexes

Two measures of stability were considered including the Showalter Index (SI) (Showalter, 1953) and the Vertical Totals Index (VT) (Miller, 1967).

The Showalter Index is obtained by raising a parcel of air dry-adiabatically from the 850-mb level to the lifting condensation level (LCL), then upward to the 500-mb level along the saturated adiabat. The Showalter Index is the difference between the temperature of the environment (T) and that of the parcel (T'), T-T', at 500 mb. When SI is +3 or less the air is quite unstable and thunderstorms may occur if other conditions are satisfied.

The VT was computed from the equation

$$VT = T_{850} - T_{500}$$

where T_{850} and T_{500} are the temperatures (°C) at 850 mb and 500 mb, respectively. In the United States, a value of 26 or higher is usually associated with the occurrence of thunderstorms except along the coastal areas of the Gulf States and over the Gulf Stream where values as small as 23 are often associated with thunderstorm activity.

c. Stratification of data

Discrepancies between satellite and rawinsonde data for all seven parameters form the computed data sets used in this research. Computations were made level-by-level (e.g., temperature), or layer-by-layer (e.g., thickness), for each sounding. In addition, the data were stratified into three layers, surface to 500 mb,

500 to 300 mb, and 300 to 100 mb. These layers are referred to as lower, middle, and upper troposphere, respectively. Statistics of the data for each layer were examined for each geographical area.

d. Computation of statistical parameters and distributions

Discrepancies were computed between satellite and rawinsonde data for the seven parameters at 21 levels for temperature, 15 levels for dew-point temperature, thicknesses for 20 layers, lapse rates of temperature for 19 levels, mixing ratios for 15 levels, precipitable water for 14 layers, and Showalter and Vertical Total Indexes for each satellite and rawinsonde sounding in each geographical area. The discrepancies, D, were defined by

$$D = (S - \overline{R})$$

where S is the satellite value and $\overline{R}$ is the corresponding weighted rawinsonde value.

For purposes of comparison, the discrepancies between layer thicknesses were normalized according to

$$D_{NZ} = \frac{D_Z}{Z_{\overline{R}}} \times 1000$$

where D_Z is the discrepancy between satellite and weighted rawinsonde layer thicknesses, and $Z_{\overline{R}}$ is the weighted rawinsonde layer thickness. Therefore, D_{NZ} is the thickness discrepancies per 1000 m (1 km).

Cumulative probability frequency distributions (CPF) of the discrepancies were computed for each layer for temperature, dew-point temperature, normalized thickness, lapse rate of temperature, and mixing ratio for the ensemble of all paired points within each layer and for the four geographical areas.

6. RESULTS

In this research, discrepancies between satellite and weighted rawinsonde data, $S-\overline{R}$, between levels or layers from the ground to 100 mb form the data sets from which the "goodness" of satellite-derived sounding data is assessed.

a. Temperature

Temperature profile data are perhaps the most basic of all information in the understanding of atmospheric structure. For this reason temperature is the first variable considered.

A satellite sounding of temperature is obtained from radiance data emanating from an area usually of considerable size. The quality of the satellite data is dependent on many aspects of the retrieval method. Because the radiance values represent areas and not points, and smoothing by the weighting functions was used, satellite-derived temperature profiles are smoothed to some extent, especially in regions where the lapse rate changes rapidly with height such as near fronts and at the tropopause. By contrast, rawinsonde data contain all significant information and provide detail of the vertical temperature structure (Horn et al., 1975).

Table 2 shows the extremes, means, standard deviations, absolute magnitudes, and root-mean-square (RMS) values of discrepancies between satellite and weighted rawinsonde temperatures over an altitude range from the surface to 100 mb for the four areas.

For Areas I, II, III, and IV, respectively, the algebraic mean discrepancies are 0.3, 0.1, 0.2, and 0.0°C with the range of 2.2 to -1.3, 0.6 to -0.7, 2.1 to -1.1, and 2.0 to -1.3°C, respectively, from which it is inferred that satellite-retrieved temperatures may be either higher or lower than rawinsonde observed temperatures, but each algebraic mean is a small positive number when averaged through the vertical column from the surface to 100 mb and over the whole area. Table 2 also shows the mean absolute discrepancies

Table 2. Selected statistics of temperature discrepancies between Nimbus 6 Satellite and weighted rawinsonde data for all four areas (°C).

	Area I			Area II			Area III			Area IV		
	Disc.	Abso. disc.	RMS	Disc.	Abso. disc.	RMS	Disc.	Abso. disc.	RMS	Disc.	Abso. disc.	RMS
Max.	2.2[1]	2.8[2]	3.2[3]	0.6	1.3	1.4	2.1	3.6	3.9	2.0	3.1	4.3
Min.	-1.3[4]	0.8[5]	1.1[6]	-0.7	0.8	0.9	-1.1	0.6	0.9	-1.3	0.9	1.3
Mean	0.3[7]	1.6[8]	2.0[9]	0.1	0.9	1.1	0.2	1.9	2.3	0.0	1.8	2.5
St. Dev.	0.7[10]	0.5[11]	0.6[12]	0.4	0.2	0.1	1.0	0.9	1.0	0.8	0.6	0.8
No. of Pairs		21			9			7			23	

1-Maximum average discrepancy for a profile pair.
2-Largest absolute discrepancy.
3-Maximum RMS of discrepancies for a profile pair.
4-Minimum average discrepancy for a profile pair.
5-Smallest absolute discrepancy.
6-Minimum RMS of discrepancies for a profile pair.
7-Average of all discrepancies for all profile pairs and all levels.
8-Average magnitude of all discrepancies for all profile pairs and all levels.
9-Average of RMS values determined for each profile pair.
10-Standard deviation of discrepancies for all profile pairs and all levels.
11-Standard deviation of the magnitude of all discrepancies for all profile pairs and all levels.
12-Standard deviation of the RMS discrepancies determined for each profile pair.

of 1.6, 0.9, 1.9, and 1.8°C for Areas I, II, III, and IV, respectively, with a range between 0.8 and 3.6°C.

Staelin et al. (1973) found similar results with discrepancies ranging between 1 and 4°C over an altitude range of 1 to 20 km. A range in RMS discrepancies between 0.9 and 4.3°C is shown in Table 2, while Waters et al. (1975) indicated RMS discrepancies between NEMS and rawinsonde data ranging between 2.5 and 4°C. The statistics in Table 2 show the best agreement between satellite and rawinsonde temperature data to be over water (Area II, Caribbean), and the worst over mountainous terrain (Area IV, western United States). While it is infeasible to show in detail the terrain features over the western United States the large changes in smoothed or average elevation are illustrated in Fig. 10.

Figures 11 through 14 give examples of the "closest" and "poorest" agreement between paired temperature profiles for each area. The four "closest" paired temperature profiles show good agreement except in the tropopause region. For example, the curves for SSM (734) (Fig. 11) agree within a reasonable noise level from 950 to 150 mb, above which there is only minor disagreement.

Those "poorest" agreement profiles shown in (b) of Figs. 11 to 14 reveal the difference between paired curves through the whole troposphere. Major disagreement is found in the layer near the tropopause between 200 to 135 mb for LBF (562) in Area I (Fig. 11), and the largest disagreements appear near the tropopause and near the ground for YYQ (913) in Area III (Fig. 13), and for DEN (469) in Area IV (Fig. 14). Over water, the "poorest" paired curves for Area II (Fig. 12) exhibit only minor disagreement through the whole column. In addition to the tropopause, the surface condition is another key factor which affects the accuracy of the satellite data. These characteristics are also shown in Tables 3 through 6 which represent the maximum absolute discrepancy between satellite and rawinsonde temperature data for each profile pair for Areas I-IV, respectively. For the central United States (Table 3), 90% of the largest discrepancies are found within the tropopause region and 10% close to the ground (850 mb). These

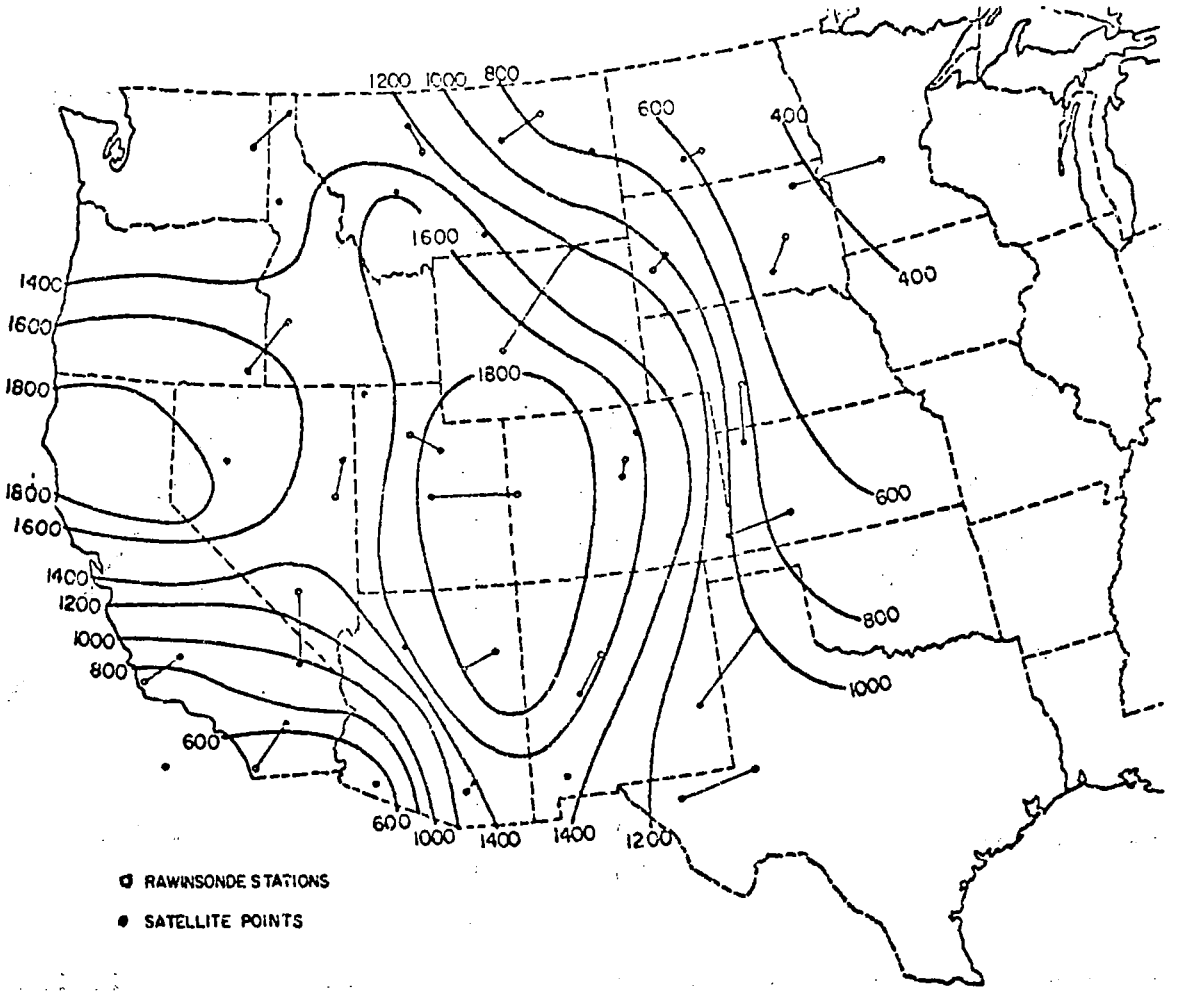

Fig. 10. Smoothed contours of average surface terrain height (m) for the western United States encompassing Area IV.

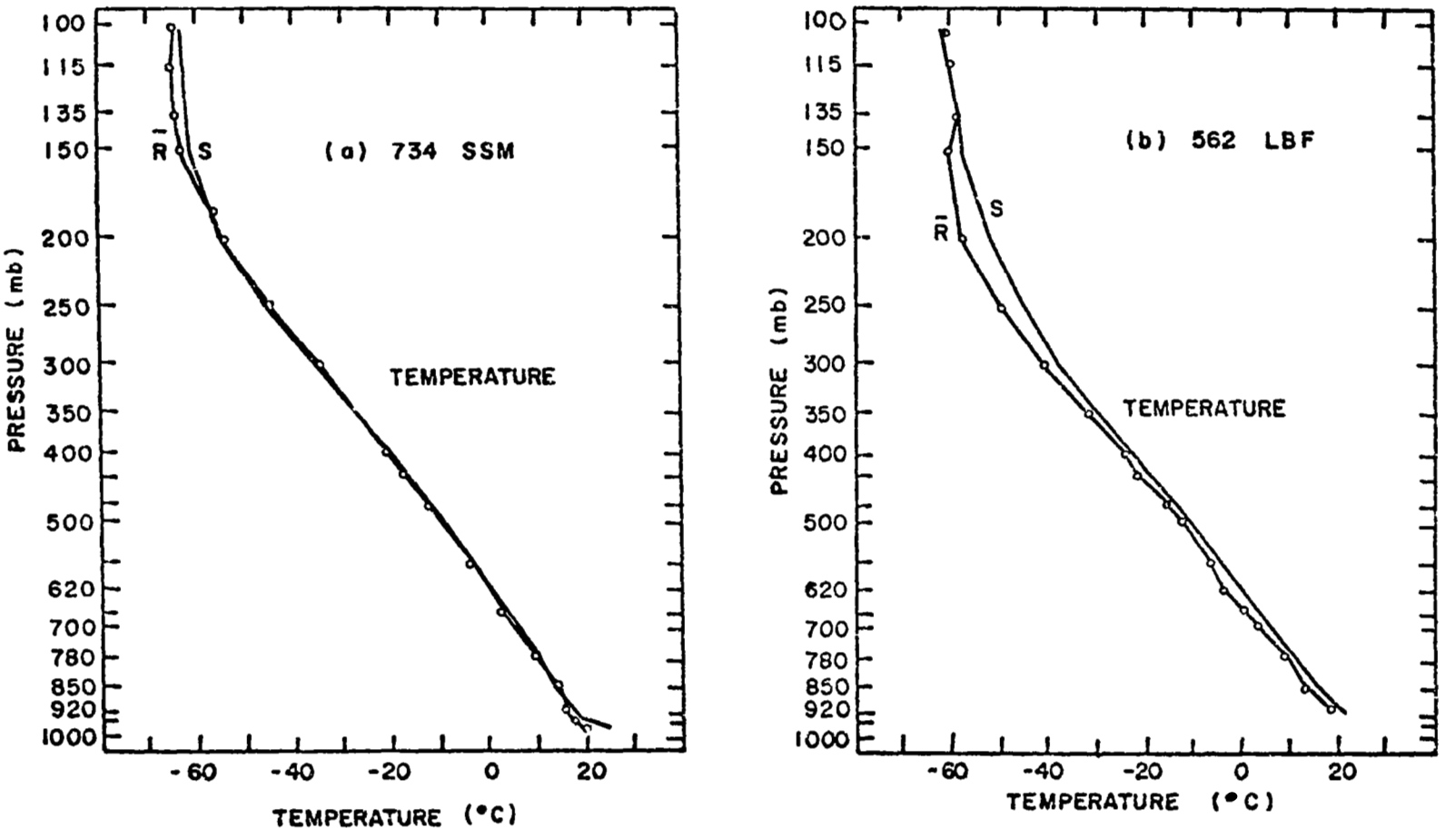

Fig. 11. Examples of the (a) "closest" and (b) "poorest" agreement between paired profiles for Area I (From Moyer, et al., 1978).

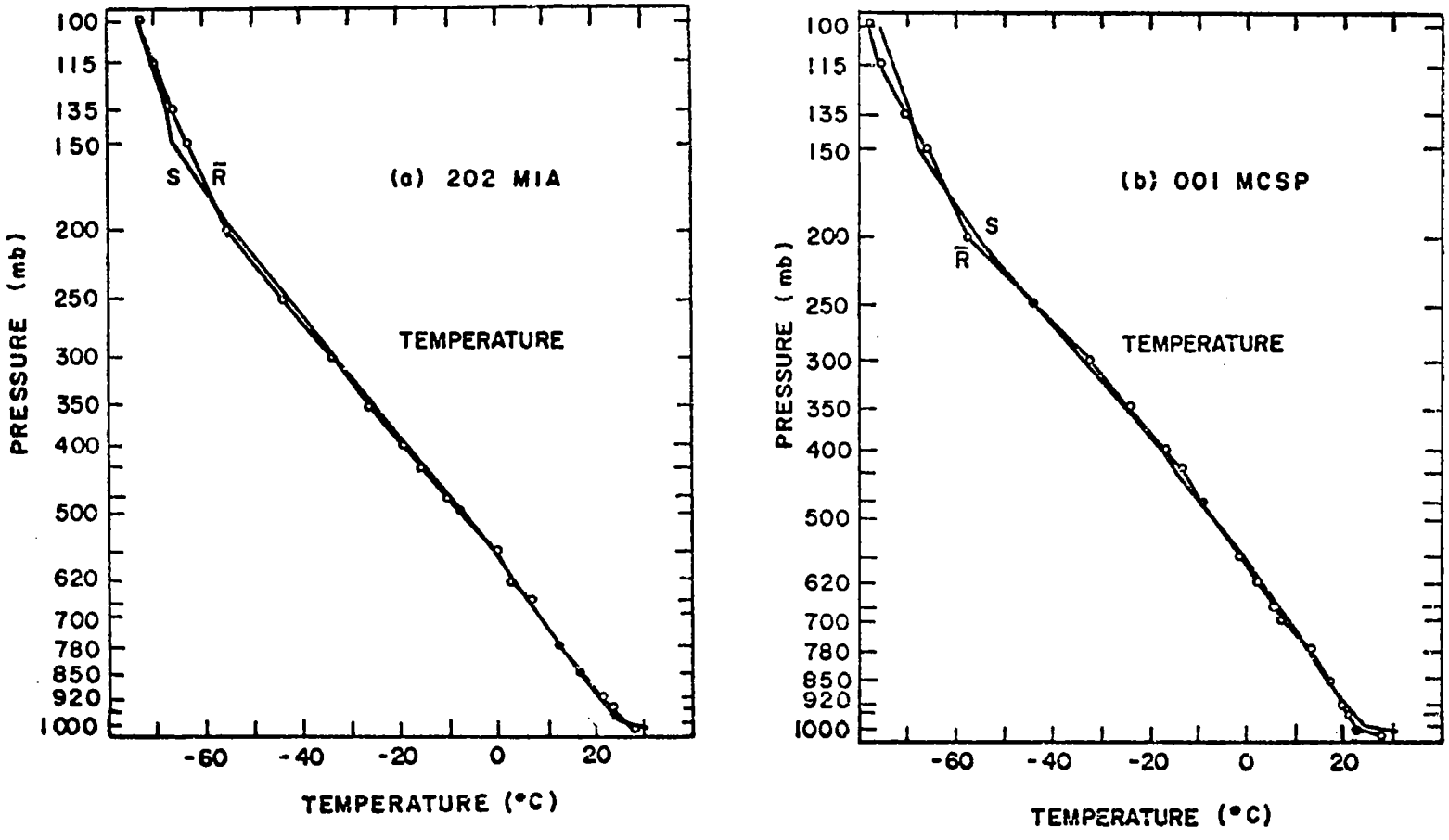

Fig. 12. Examples of the (a) "closest" and (b) "poorest" agreement between paired profiles for Area II.

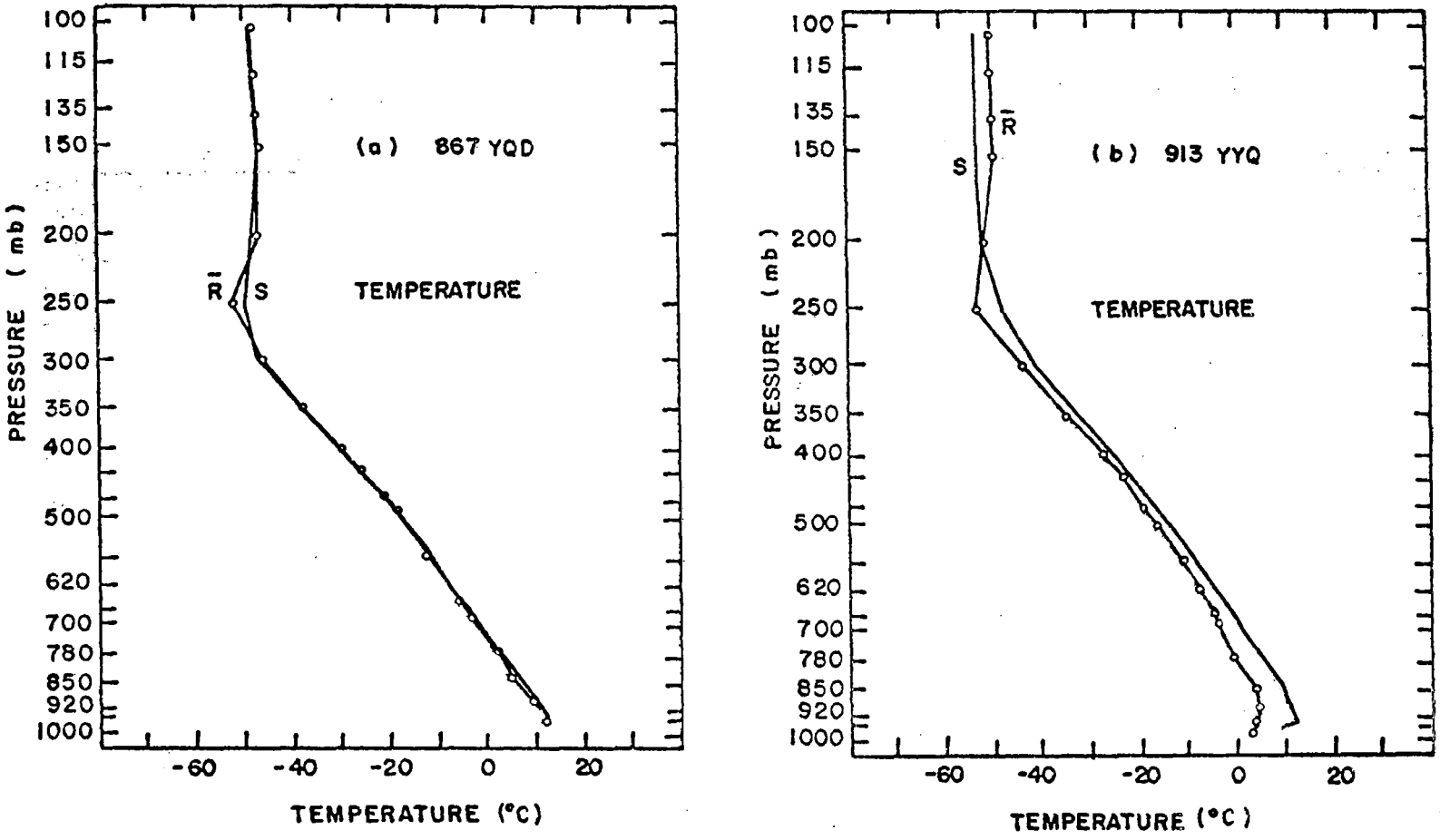

Fig. 13. Examples of the (a) "closest" and (b) "poorest" agreement between paired profiles for Area III.

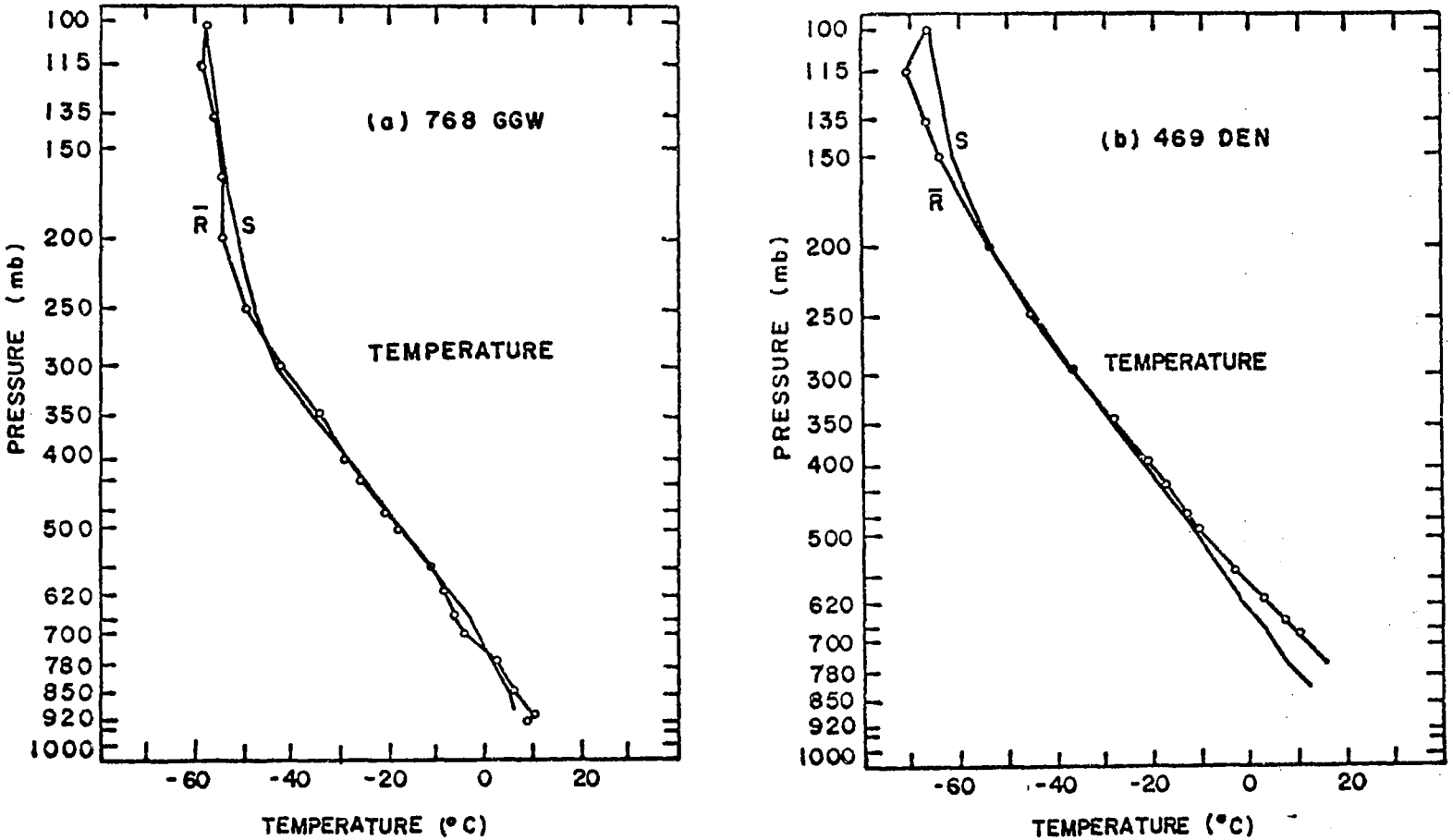

Fig. 14. Examples of the (a) "closest" and (b) "poorest" agreement between paired profiles for Area IV.

Table 3. Maximum absolute discrepancy between Nimbus 6 and rawinsonde temperatures for each profile pair for Area I (°C).

STATION	MAXIMUM (deg)	PRESSURE LEVEL (mb)
229	4.2	115
235	2.4	850
247	3.4	115
260	4.0	135
311	5.1	115
327	4.2	115
340	5.5	115
349	7.1	115
353	4.5	300
429	5.5	115
433	5.6	135
451	MSG	MSG
456	4.9	135
532	5.5	135
553	4.1	115
562	5.9	200
645	6.0	115
654	2.8	200
655	3.3	850
734	2.6	135
747	3.1	200

Table 4. Maximum absolute discrepancy between Nimbus 6 and rawinsonde temperatures for each profile pair for Area II (°C).

STATION	MAXIMUM (deg)	PRESSURE LEVEL (mb)
201	1.7	475
202	2.1	150
210	1.9	950,200
644	3.4	100
367	2.2	950,200
397	2.8	115
501	2.4	620
806	2.2	1000
001	2.6	200

Table 5. Maximum absolute discrepancy between Nimbus 6 and rawinsonde temperatures for each profile pair for Area III (°C).

STATION	MAXIMUM (deg)	PRESSURE LEVEL (mb)
768	4.2	850
836	9.2	150
848	3.3	780
867	2.2	250
913	6.8	950,920
934	4.5	780
119	2.9	850

Table 6. Maximum absolute discrepancy between Nimbus 6 and rawinsonde temperatures for each profile pair for Area IV (°C).

STATION	MAXIMUM (deg)	PRESSURE LEVEL (mb)
265	5.4	200
274	7.0	850
290	5.8	780
363	3.7	850
365	6.3	780
374	5.3	780
385	4.4	850
393	5.5	115
451	5.5	850
469	7.7	780
476	10.0	780
486	7.3	780
562	4.6	500,300
572	6.8	780
576	6.0	100
654	5.8	950
655	7.0	135
662	4.5	115
681	4.2	250
764	4.0	115
768	2.7	200
775	5.3	850
785	4.2	200

discrepancies range between 2.4°C at 850 mb to 7.1°C at 115 mb. In Area II (see Table 4) smaller values occurred with a range between 1.7°C at 475 mb and 3.4°C at 100 mb. In this area no obvious regular pattern is indicated by the data, but a high percentage of the largest discrepancies occurred in the tropopause region. In the Canadian area (Area III), Table 5 shows that 70% of the maximum discrepancies are found near the ground, and 30% in the tropopause region. The range of values is large and varies between 2.2°C at 250 mb and 9.2°C at 150 mb. Table 6 shows for the western United States (Area IV) approximately the same percentage frequency of the largest values but with a higher percentage close to the ground than in Area III. In Area IV the maximum discrepancies range between 2.7°C at 200 mb and 10.0°C at 780 mb. This is the largest range for any of the four areas. From a comparison of all four areas, it can be concluded that the largest discrepancies between satellite and rawinsonde sounding data occur in the tropopause region or near the surface. Staelin et al. (1973) have shown similar results, and Smith et al. (1975) have shown that in the troposphere the discrepancies between satellite and rawinsonde soundings were generally small except in the tropopause region between 300 to 100 mb. Their results are in agreement with those presented in this study.

Over the western United States (Table 6), 50% of the largest discrepancies are found near the ground, while over the Caribbean (Table 4), the discrepancies at all altitudes are relatively small by comparison with other areas. These differences apparently are due to the different surface conditions, i.e., mountains in Area IV and water in Area II.

Figure 15 shows temperature discrepancies, $(S - \overline{R})$, for stations 260, 433, and 734 in Area I, for stations 202 and 001 in Area II, for stations 836 and 913 in Area III, and for stations 274, 476, and 654 in Area IV. Data for these stations illustrate the main characteristics of the discrepancies mentioned above for the four areas.

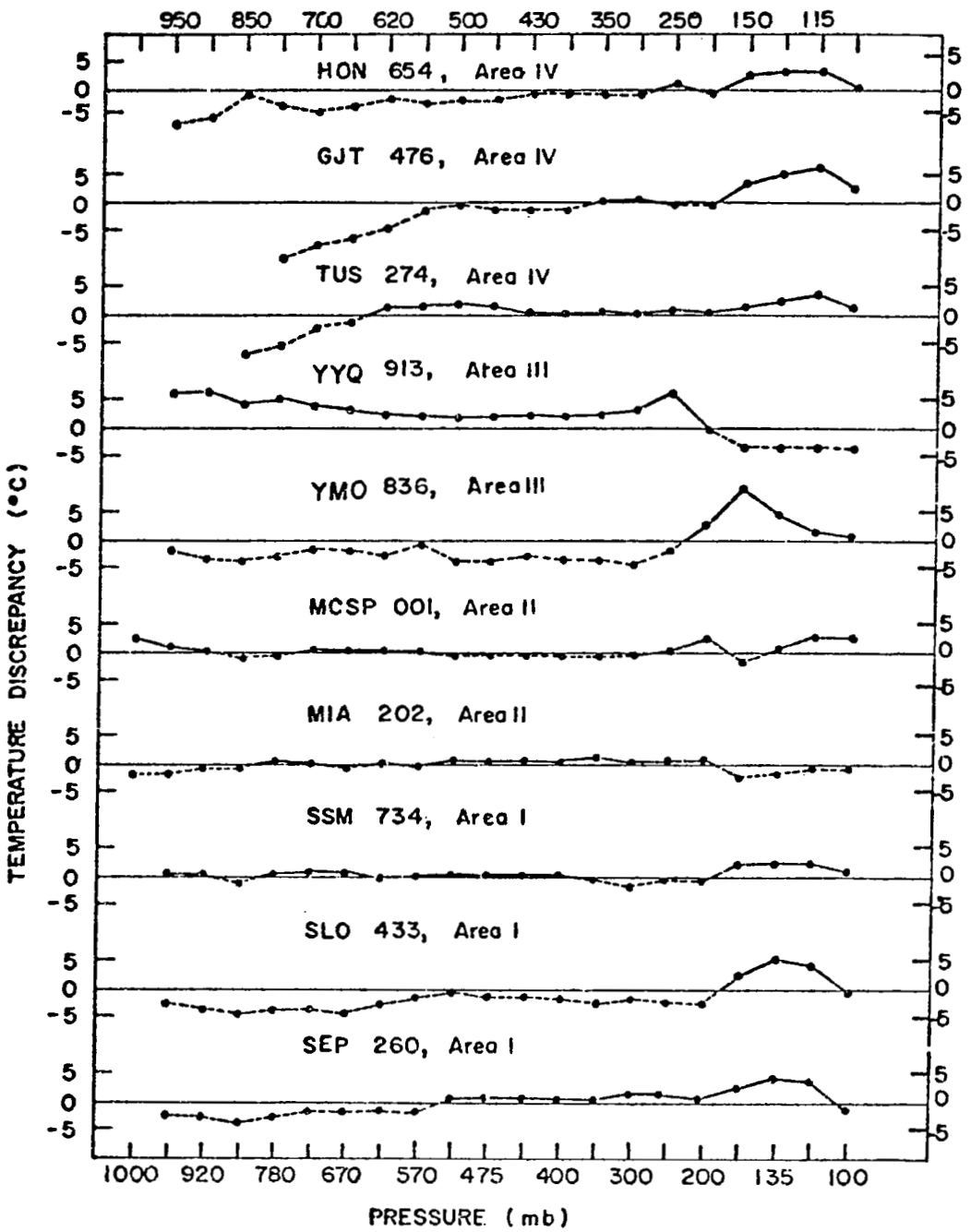

Fig. 15. Temperature discrepancies between satellite and rawinsonde data as a function of pressure for selected stations in each of the four geographical areas.

The results presented above show that the magnitudes of the temperature discrepancies vary with altitude and the type of surface, but do not address the questions of how the statistics of the discrepancies vary with altitude and what are their statistical distributions. These questions were addressed by stratifying the discrepancies by layer, i.e., surface to 500 mb, 500 to 300 mb, and 300 to 100 mb. These layers will be referred to as the lower, middle, and upper troposphere, and denoted by A, B, and C, respectively. Each layer contains a sufficient number of data points for statistical analyses which was the primary purpose for stratification of the data.

The mean, standard deviation, and cumulative frequency distribution of the discrepancy data within each layer for temperature, dew-point temperature, mixing ratio, normalized thickness, and lapse rate of temperature were calculated for each area. The means and standard deviations of temperature discrepancies for all layers and areas are shown in Table 7, and the cumulative frequency distributions plotted on probability paper are shown in Figs. 16 through 19.

The algebraic means listed in Table 7 indicate that the negative biases between satellite and rawinsonde temperature data are found in the lower troposphere (surface to 500 mb), with the exception of a mean of 0.1°C for the Canadian area. Very small mean values of the discrepancies for Areas I, II, and III are shown, which indicates a good correspondence in the means between satellite and rawinsonde temperature data, although for Area IV there is a negative bias of -1.6°C. This means that the average satellite temperature was 1.6°C lower than the average weighted rawinsonde temperature in this layer.

The positive biases (average satellite temperature higher than average rawinsonde temperature) are found systematically both in the middle and upper troposphere (500 to 300 mb, and 300 to 100 mb) with values generally positive but less than 1°C with the exception of a mean of -0.4°C in the middle layer for the Canadian area (Area III). Curves in Fig. 15 also show that satellite

Table 7. Mean and standard deviation of temperature discrepancies (°C) between Nimbus 6 satellite and weighted rawinsonde data stratified by three layers: (A) Surface to 500 mb; (B) 500 to 300 mb; (C) 300 to 100 mb.

	Area I			Area II			Area III			Area IV		
	A	B	C	A	B	C	A	B	C	A	B	C
Mean (°C)	-0.5	0.5	1.3	-0.1	0.5	0.3	0.1	-0.4	0.8	-1.6	0.0	1.8
St. Dev. (°C)	1.8	1.3	2.3	1.1	0.8	1.3	2.5	2.0	2.5	2.6	1.5	1.9
No. of data	189	124	140	90	54	55	61	42	49	160	138	157

temperature is lower than rawinsonde temperature in the layer near the ground with opposite conditions in both the middle and upper tropospheric layers.

The standard deviations of 1.8, 1.1, 2.5, and 2.6°C are listed in the table for Areas I, II, III and IV, respectively. The smallest standard deviation occurs over water (Area II), and the larger over Canada (Area III) and the western United States (Area IV). Also, in each area the smallest value occurs in the middle troposphere, with the largest value in the upper troposphere, i.e., tropopause region, except for Area IV.

The cumulative frequency distributions shown in Figs. 16, 17, 18, and 19 are approximately normal (straight lines) except near the extremes. This is probably caused by the small data samples which are inadequate for defining the extremes of the distributions. The distributions in Fig. 18 are more irregular than those in Figs. 16, 17, and 19. This may be due to the small number of data used to determine the distributions. Even in these cases the assumption of a normal distribution appears reasonable. The tendency for the cumulative frequency distributions to be straight lines when plotted on probability paper suggests that the discrepancies between satellite and rawinsonde temperatures are due to random errors relative to any biases that may be present

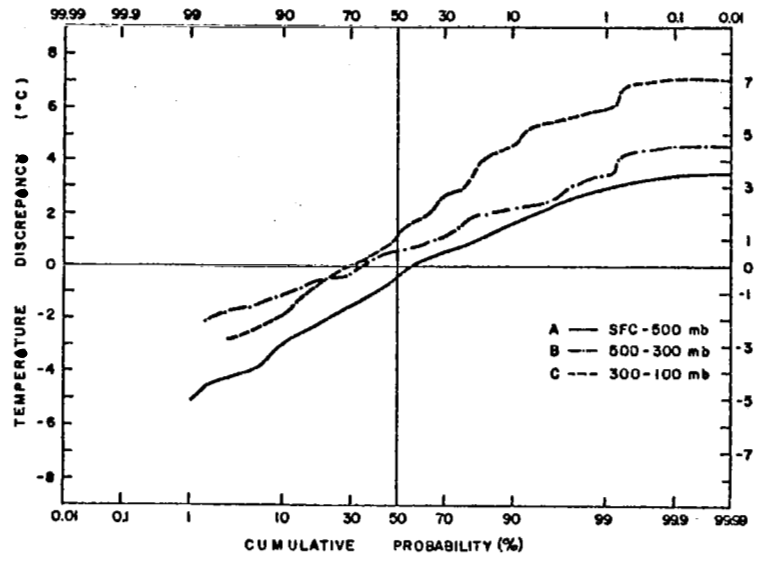

Fig. 16. Cumulative frequency distributions of discrepancies in temperature in the layers surface to 500 mb, 500 to 300 mb, and 300 to 100 mb for Area I (central United States).

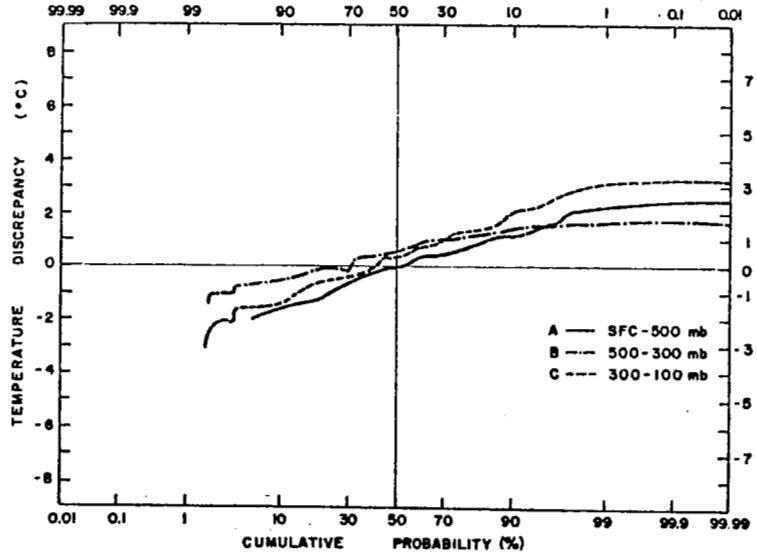

Fig. 17. Cumulative frequency distributions of discrepancies in temperature in the layers surface to 500 mb, 500 to 300 mb, and 300 to 100 mb for Area II (Caribbean).

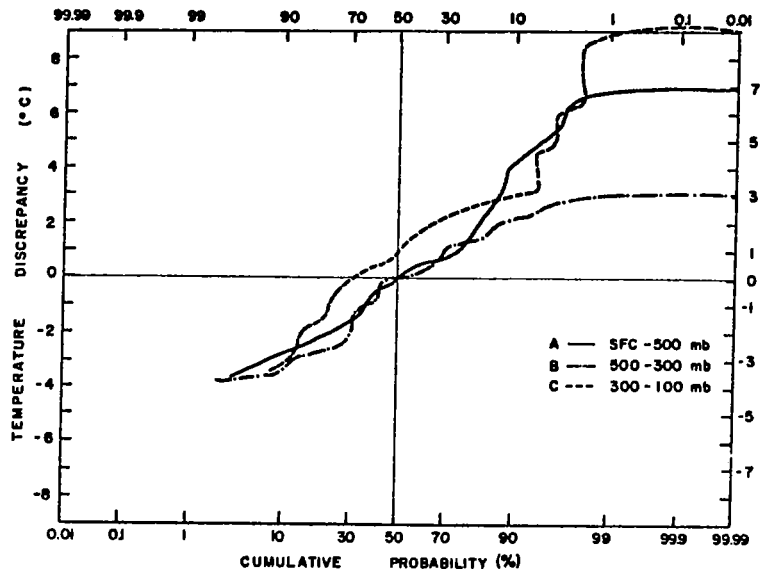

Fig. 18. Cumulative frequency distributions of discrepancies in temperature in the layers surface to 500 mb, 500 to 300 mb, and 300 to 100 mb for Area III (Canada).

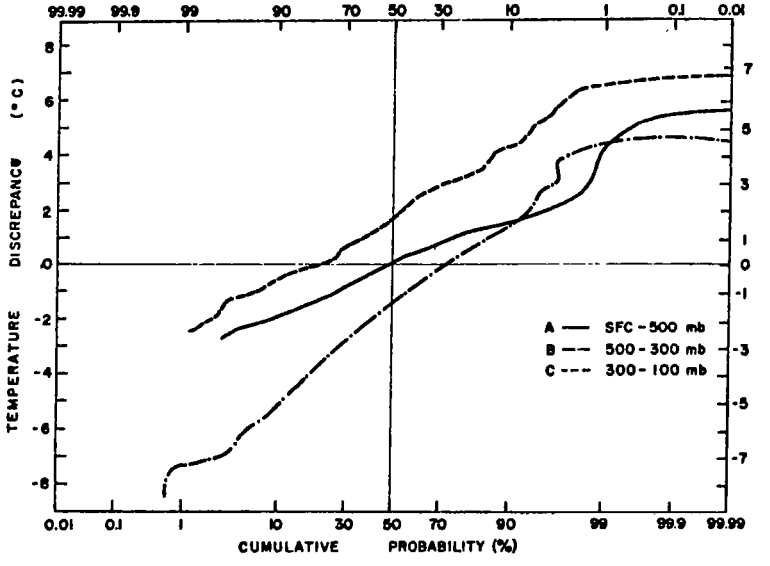

Fig. 19. Cumulative frequency distributions of discrepancies in temperature in the layers surface to 500 mb, 500 to 300 mb, and 300 to 100 mb for Area IV (western United States).

in either type of data. If a correction were made for the bias in a given layer the statistical distribution would be unaffected although the standard deviation would be reduced.

b. Dew-point temperature

The Nimbus 6 HIRS and SCAMS soundings of dew-point temperature do not appear to be as reliable as those of temperature for any of the four areas. Table 8 shows the mean discrepancies and mean RMS discrepancies for the vertical column surface to 300 mb for the four areas. The mean RMS discrepancies range between 6.6°C (Area II) and 9.1°C (Area IV). The greatest disagreement is found for the western United States, which may be attributed to the type of air mass sampled or terrain influences. The air masses over the central United States above the 700-mb level and over the Caribbean area were maritime tropical, over the Canadian area the air mass was mixed tropical and polar air that formed the occluded part of the cold front, while that above the western United States was superior (dry) air. Because of the extremely low water vapor content of the air over the western United States, the data were considerably more variable.

Table 8. Means and standard deviations of discrepancies and the root-mean-square of discrepancies between satellite and weighted rawinsonde dew-point temperatures for Areas I, II, III, and IV (°C).

	Area I		Area II		Area III		Area IV	
	Disc	RMS	Disc	RMS	Disc	RMS	Disc	RMS
Mean	2.9	7.3	2.8	6.6	-2.0	6.8	6.0	9.1
St. Dev.	3.8	2.5	3.1	2.6	4.6	2.2	5.7	4.7
No. of pairs	21		9		7		23	

Discrepancies in dew point temperatures were examined for the layers surface to 500 mb, and 500 to 300 mb. Means and standard deviations of the discrepancies within the two layers for all four

areas are shown in Table 9. Cumulative frequency distributions of the discrepancies for each layer and area are presented in Figs. 20 through 23. Table 9 also shows the large biases (mean differences) in the Nimbus 6 dew-point temperatures. In all areas, the mean difference is smaller in the lower layer than in the upper layer. This may be attributable to the higher moisture content in the lower layer than that in the upper layer where the data were considerably noisier than in the lower layer. The large standard deviations indicate large dispersions of the discrepancies and imply large ranges for each layer. The cumulative frequency distributions in Figs. 20 through 23 reflect the large dispersion by their large slopes. They also show that the discrepancies in dew point do not follow a normal distribution nearly as well as the temperature discrepancies. A contribution to the discrepancies arises from errors in the rawinsonde sensors, but the primary contribution is believed to be in the satellite data since their reliability is highly questionable.

Table 9. Means and standard deviations of discrepancies in dew-point temperature within the layers surface to 500 mb, and 500 to 300 mb for all four areas (°C).

	Area I		Area II		Area III		Area IV	
	A	B	A	B	A	B	A	B
Mean	1.6	4.7	1.7	5.8	-2.0	-2.2	4.9	7.7
St. Dev.	5.8	8.7	6.2	7.0	5.2	9.0	7.8	9.7
No. of data	189	120	89	51	60	32	157	127

c. Thickness

The analysis of discrepancies between Nimbus 6 and weighted rawinsonde data for temperature and dew-point temperature are presented in previous sections. In this and following sections, several computed variables based on temperature and dew-point temperature are examined. The first of these is thickness, the

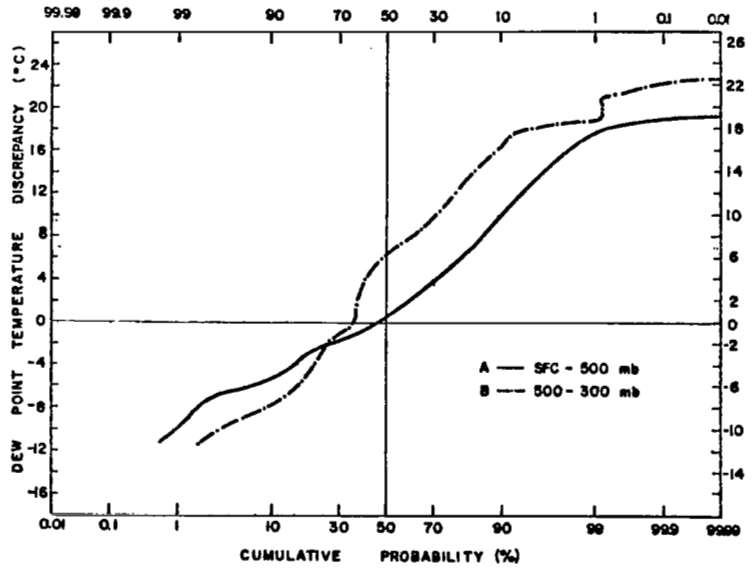

Fig. 20. Cumulative frequency distributions of discrepancies in dew-point temperature in the layers surface to 500 mb, and 500 to 300 mb for Area I (central United States).

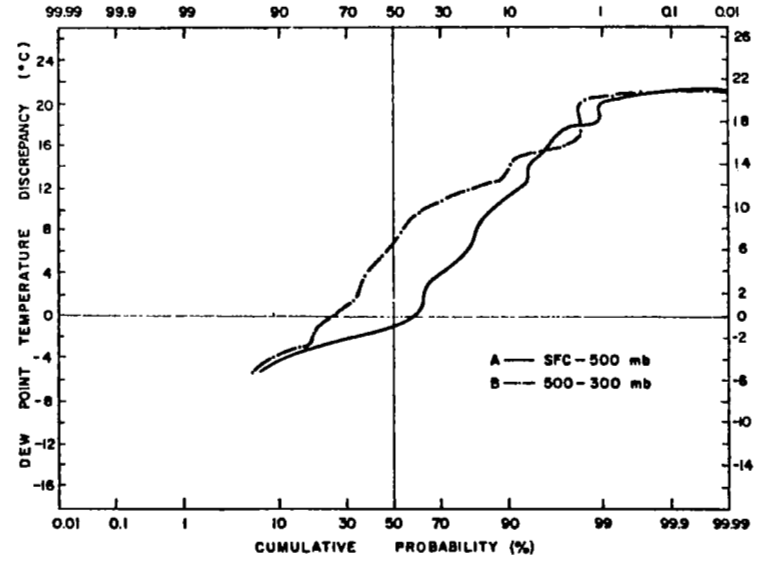

Fig. 21. Cumulative frequency distributions of discrepancies in dew-point temperature in the layers surface to 500 mb, and 500 to 300 mb for Area II (Caribbean).

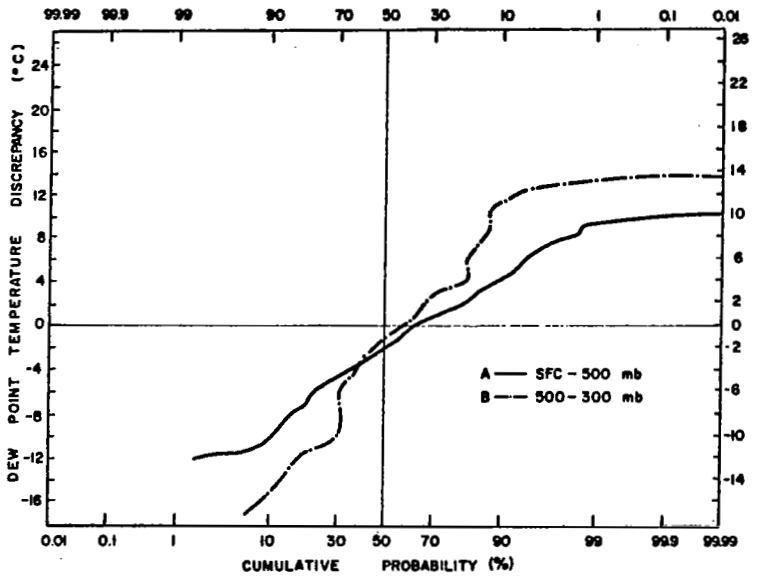

Fig. 22. Cumulative frequency distributions of discrepancies in dew-point temperature in the layers surface to 500 mb, and 500 to 300 mb for Area III (Canada).

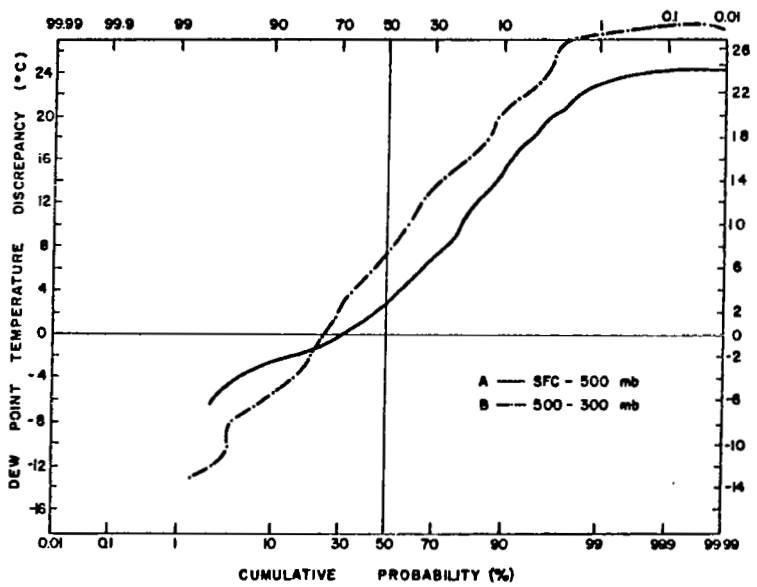

Fig. 23. Cumulative frequency distributions of discrepancies in dew-point temperature in the layers surface to 500 mb, and 500 to 300 mb for Area IV (western United States).

equations for which were given in the section on data analysis.

The means and standard deviations of the discrepancies between Nimbus 6 satellite and weighted rawinsonde layer thicknesses determined from mean ambient temperature and mean virtual temperature for the 20 layers contained in each profile from the surface to 100 mb and for all four areas, are shown in Table 10. The statistics of the discrepancies between thicknesses determined from mean virtual temperature are larger than the values determined from mean ambient temperature, but the differences are small. Therefore, the effects of inaccurate measurements of satellite moisture on computed thickness is small and the average amounts to approximately 2%.

Since the satellite temperatures are higher than rawinsonde temperatures on the average (Table 2), the mean discrepancies shown in Table 10 are positive for all four areas. The mean RMS discrepancy for thickness ranges between 3.51 m for Area II and 8.95 m for Area IV. These discrepancies correspond to a range of mean RMS temperature discrepancies of 1.1°C for Area II to 2.5°C for Area IV. The data in Table 10, like those in Table 2, show that the best agreement is found over water (Area II) and the poorest agreement over mountains (Area IV).

The statistics presented in Table 10 for the layer from the surface to 100 mb reveal no information about the statistics of the discrepancies as a function of altitude. Therefore, the statistics of the thicknesses were examined for three layers: surface to 500 mb; 500 to 250 mb; and 250 to 100 mb. Means and standard deviations of the discrepancies between satellite and weighted rawinsonde thicknesses for the three layers and for the four areas are shown in Table 11. Also shown in Table 11 are values obtained by Wilcox and Sanders (1976) for comparison with the data obtained in this study. They computed thicknesses for the layers 1000-500 mb, 500-250 mb, and 250-50 mb over low-latitude ocean areas, mid-latitude land, and high-latitude land. The results from the present study are for the layers surface-500 mb, 500-250 mb, and 250-100 mb. In Table 11, the results for the Caribbean area are compared with

those for the low-latitude ocean, those for the central and western United States are compared with mid-latitude land, and results from Canada are compared with high-latitude land.

Table 10. Means and standard deviations of thickness discrepancies determined from thicknesses computed from mean temperature and mean virtual temperature for all four areas (m). The statistics were computed from data for all layers from the surface to 100 mb.

	Area I		Area II		Area III		Area IV	
	$\overline{T}$	$\overline{T}^*$	$\overline{T}$	$\overline{T}^*$	$\overline{T}$	$\overline{T}^*$	$\overline{T}$	$\overline{T}^*$
Mean	1.68	1.73	0.94	0.95	1.30	1.26	1.99	2.14
St. Dev.	2.74	2.76	0.85	0.98	2.11	2.19	2.89	2.96
RMS	7.72	7.76	3.51	3.62	7.77	7.81	8.95	8.90
St. Dev.	2.52	2.57	0.56	0.65	4.32	4.39	2.35	2.38
No. of pairs	21		9		7		23	

The results for the Caribbean for both the mean and standard deviation are much smaller than those for low-latitude oceans, and the algebraic signs of mean discrepancies are opposite for the lower and middle layers for the two studies. In the second part of Table 11 (mid-latitude land), the algebraic signs of mean discrepancies are also opposite for the two studies. Moreover, the standard deviations obtained in the present study for the central and western United States are much smaller than those for mid-latitude land. The signs of the mean of the discrepancies for Canada and high-latitude land also are opposite in the two studies. The reasons for these differences between the two studies are unknown.

Results from the present study show a certain amount of consistency between areas. For example, all areas show negative average discrepancies in the layer near the ground, positive values for the layer from 500 to 250 mb except the Canadian area, and large positive values for the uppermost layer.

Table 11. Means and standard deviations of discrepancies between (a) Nimbus 5 satellite and rawinsonde, and (b) Nimbus 6 satellite and rawinsonde layer thicknesses (m). (Nimbus 5 results taken from Wilcox and Sanders, 1976)

	Layer	Mean	St. Dev.	No. of Cases
(a) Low-latitude oceans (equator to 30°)	1000-500 mb	0.9	19.8	9
	500-250 mb	-43.4	30.5	10
	250- 50 mb	45.2	55.1	6
(b) Caribbean	SFC-500 mb	-0.4	13.4	9
	500-250 mb	10.7	12.0	9
	250-100 mb	7.9	12.8	7
(a) Mid-latitude land (30° to 55°)	1000-500 mb	3.5	37.4	41
	500-250 mb	-2.9	46.3	41
	250- 50 mb	-71.3	142.9	13
(b) Central U. S.	SFC-500 mb	-8.1	26.7	21
	500-250 mb	8.1	25.9	20
	250-100 mb	33.3	32.2	20
Western U. S.	SFC-500 mb	-20.6	22.6	23
	500-250 mb	6.5	23.8	23
	250-100 mb	54.0	25.5	22
(a) High-latitude land (55° to 80°)	1000-500 mb	-7.9	39.4	48
	500-250 mb	27.4	42.1	45
	250- 50 mb	-180.5	123.5	15
(b) Canada	SFC-500 mb	-0.1	38.3	7
	500-250 mb	-2.0	41.1	7
	250-100 mb	26.3	40.0	7

As was done in the analysis of temperature and dew-point temperature, layer thickness discrepancies also were stratified into three layers, i.e., surface to 500 mb, 500 to 300 mb, and 300 to 100 mb. The thickness discrepancies were normalized to units of m km^{-1} because of the variable thickness of the layers. The means and standard deviations of normalized discrepancies in

thickness are presented in Table 12. The data in this table are similar to those for temperature shown in Table 7.

The best agreement between satellite and rawinsonde-derived thicknesses occurs in the middle layer, and the poorest in the upper layer (tropopause region). The smallest discrepancies occurred over water (Area II), and the largest over the western United States and Canada. These results also can be identified in the cumulative probability curves shown in Figs. 24 through 27. Biases of about ±2 m km^{-1} are indicated for the lower and middle layers of Areas I, II, and III in Figs. 24, 25, and 26, respectively, and a large bias of -5.4 m is found in Area IV (Fig. 27) for the lower layer where variations in topography caused larger errors near the ground. The large standard deviations for the upper layers of the four areas are reflected by the large slopes of the curves.

Table 12. Means and standard deviations of normalized discrepancies in thickness for the layers surface to 500 mb, 500 to 300 mb, and 300 to 100 mb for all areas (m).

	Area I			Area II			Area III			Area IV		
	A	B	C	A	B	C	A	B	C	A	B	C
Mean	-1.8	1.9	6.0	-0.3	1.9	1.5	0.3	-1.5	3.6	-5.4	-0.4	8.1
St. Dev.	6.2	4.8	10.0	3.3	2.8	4.6	8.9	7.5	10.1	8.1	5.7	8.3
No. of data	169	124	140	81	54	54	54	42	49	138	138	157

d. Mixing ratio

In this study, mixing ratios were obtained from plotted skew T-log p diagrams for each of the 21 data levels for each sounding from the surface to 300 mb. A mean RMS discrepancy of 1.34 g kg^{-1} was found for the ensemble of all four areas and all levels. Because of the high variability and usual decrease in the amount of water vapor with height through the troposphere, mixing ratio data were stratified into two layers; surface to 500 mb, and 500

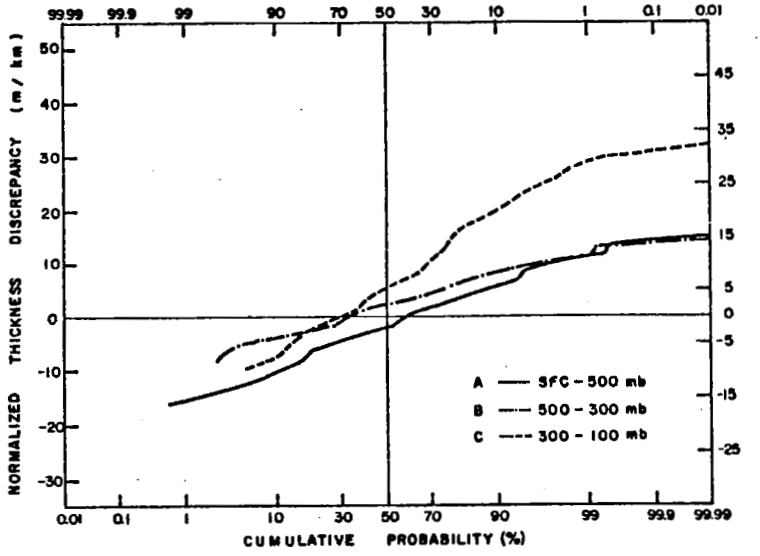

Fig. 24. Cumulative probability frequency distributions of normalized thickness discrepancies within the layers surface to 500 mb, 500 to 300 mb, and 300 to 100 mb for the central United States (Area I).

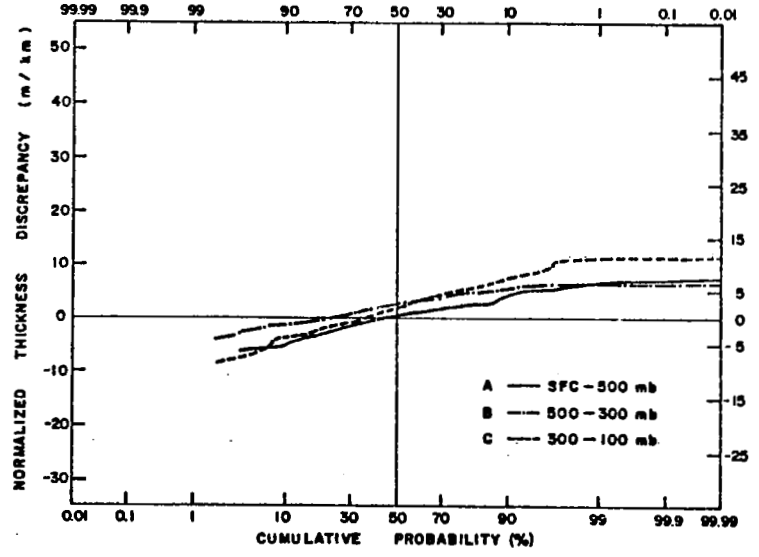

Fig. 25. Cumulative probability frequency distributions of normalized thickness discrepancies within the layers surface to 500 mb, 500 to 300 mb, and 300 to 100 mb for the Caribbean (Area II).

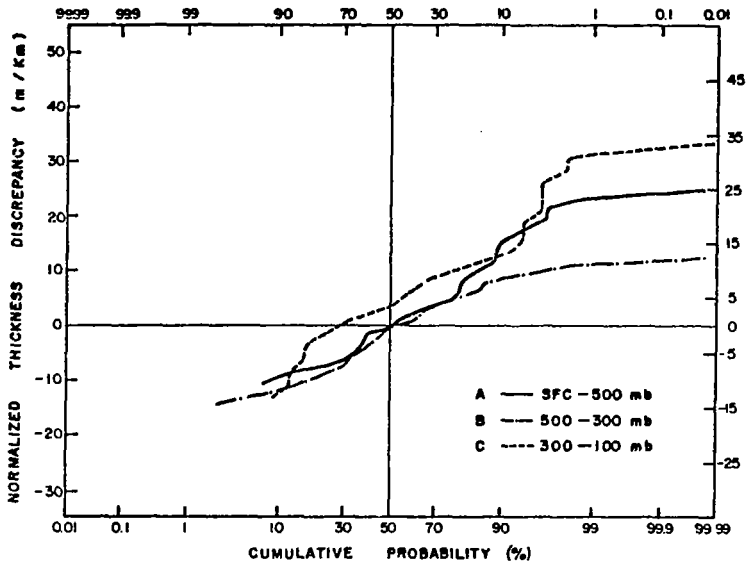

Fig. 26. Cumulative probability frequency distributions of normalized thickness discrepancies within the layers surface to 500 mb, 500 to 300 mb, and 300 to 100 mb for Canada (Area III).

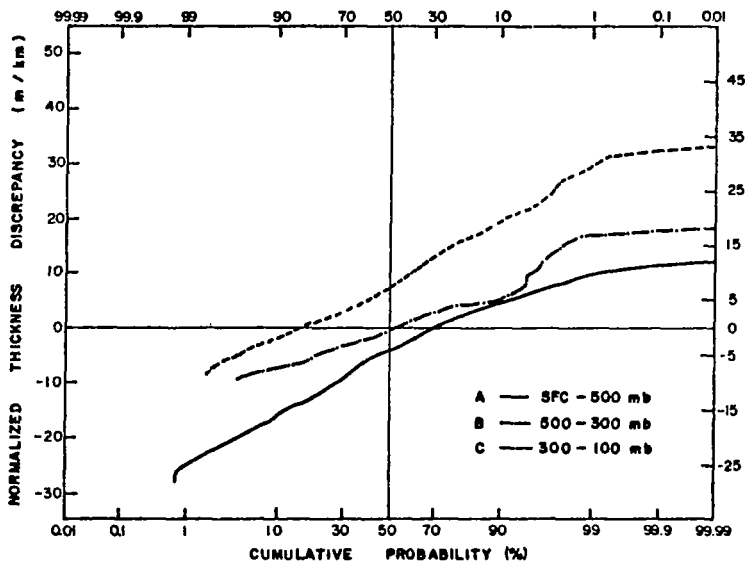

Fig. 27. Cumulative probability frequency distributions of normalized thickness discrepancies within the layers surface to 500 mb, 500 to 300 mb, and 300 to 100 mb for the western United States (Area IV).

to 300 mb. The results are presented in Table 13. The means and standard deviations of the discrepancies in the lower layers are greater than those in the upper layer for all areas. These results were due to the lower moisture content in the upper layer where the data were considerably noisier than in the lower layer. The negative biases of -0.35, -0.29 and -0.03 g kg^{-1}, which indicate less moisture in the satellite soundings than in the rawinsonde soundings, occurred in the lower layer of Areas II and III, and the upper layer of Area III, respectively. Differences in sign remain unexplained.

Table 13. Mean and standard deviations of discrepancies (g kg^{-1}) between Nimbus 6 satellite and weighted rawinsonde mixing ratio data stratified into two layers: (A) surface to 500 mb and (B) 500 to 300 mb.

	Area I		Area II		Area III		Area IV	
	A	B	A	B	A	B	A	B
Mean	0.17	0.14	-0.35	0.23	-0.29	-0.03	0.79	0.22
St. Dev.	1.84	0.61	2.10	0.58	1.50	0.25	1.47	0.52
No. of data points	189	120	90	52	61	33	159	127

Figures 28 through 31 show the relative cumulative frequency distributions for the data in Table 13. The range of the discrepancy data in the lower layer is greater than that in the upper layer for each area. Again, this resulted from the noisier satellite data associated with the lower moisture content in the upper layer. Except near the tails, the curves represent normal distributions. The statistics in Table 13 agree closely with the curves in Figs. 28 through 31.

As was the case in the analysis of discrepancies in dew-point temperature, systematic differences between satellite and rawinsonde

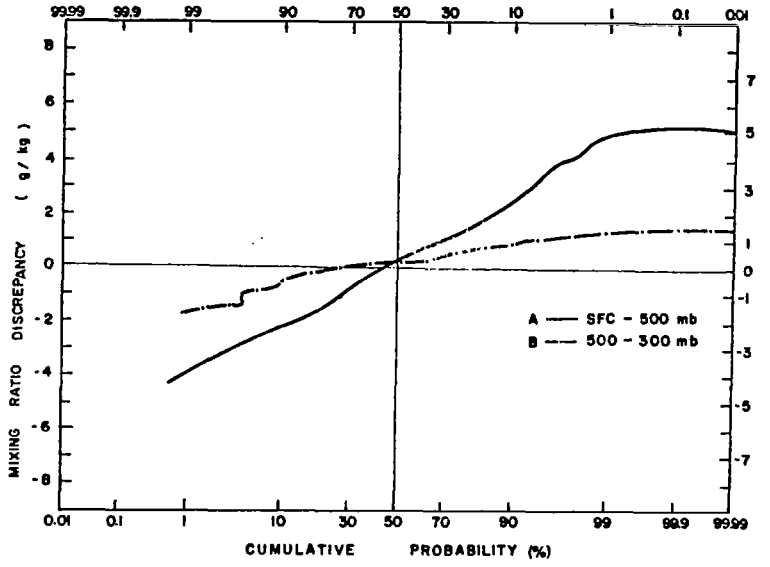

Fig. 28. Cumulative frequency distributions of discrepancies in mixing ratio in the layers surface to 500 mb, and 500 to 300 mb for the central United States (Area I).

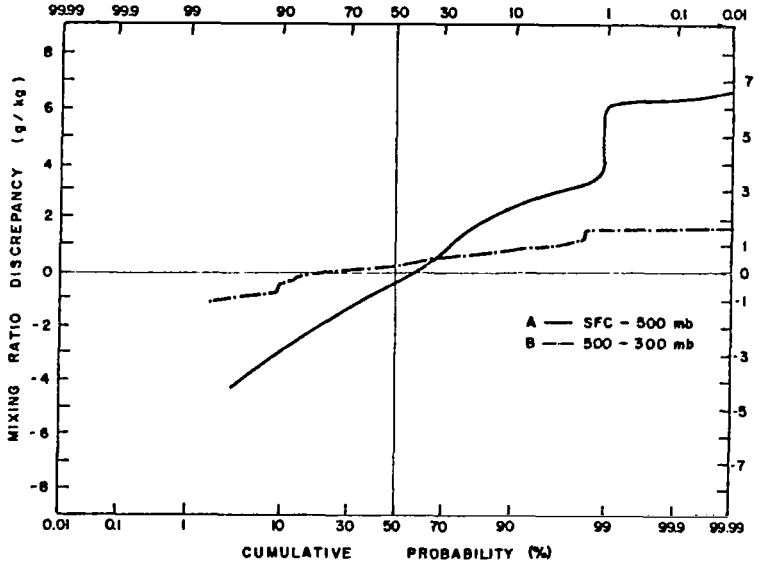

Fig. 29. Cumulative frequency distributions of discrepancies in mixing ratio in the layers surface to 500 mb, and 500 to 300 mb for the Caribbean (Area II).

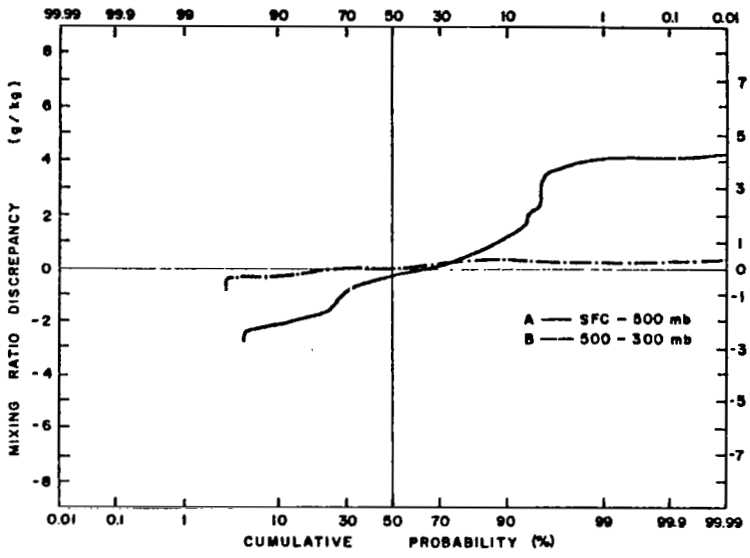

Fig. 30. Cumulative frequency distributions of discrepancies in mixing ratio in the layers surface to 500 mb, and 500 to 300 mb for Canada (Area III).

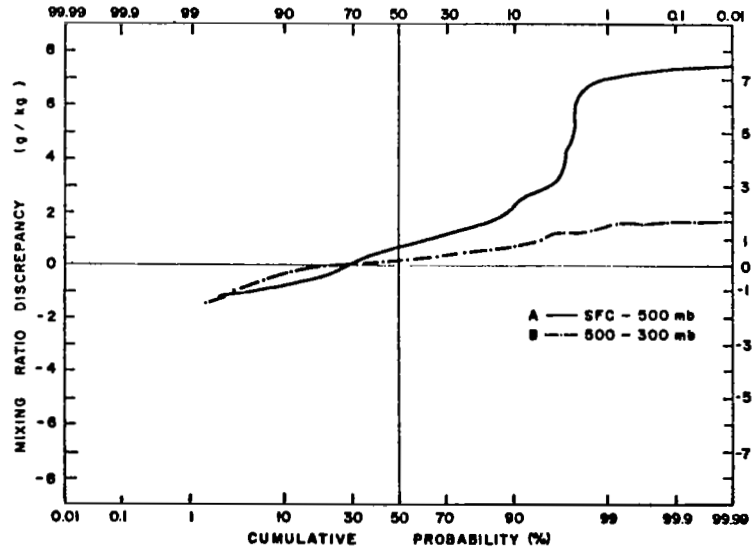

Fig. 31. Cumulative frequency distributions of discrepancies in mixing ratio in the layers surface to 500 mb, and 500 to 300 mb for the western United States (Area IV).

mixing ratios were not found for any of the four areas. The reliability of the satellite mixing ratio data is questionable.

e. Precipitable water

In addition to mixing ratio, precipitable water is another measure of atmospheric water content. In this study, precipitable water was computed by integrating the moisture profile from the surface to 300 mb. A mean RMS discrepancy between profile pairs for all four areas of only 0.23 cm was found. This is somewhat better than the 0.5 cm RMS found by Hillger and Von der Haar (1977), presumably because of the microwave channels available on Nimbus 6.

Means and standard deviations of discrepancies in precipitable water for the four areas are shown in Table 14. The results show that average precipitable water may be obtained from satellite data with an accuracy of about 0.1 cm or less which is quite acceptable in most cases. In two areas the means were negative, and in two they were positive. The standard deviations were quite consistent with a value around 0.23 except for Area IV (western United States) where the moisture content was low.

Table 14. Means and standard deviations of discrepancies (cm) between Nimbus 6 satellite and weighted rawinsonde precipitable water for all four areas.

	Area I	Area II	Area III	Area IV
Mean	0.07	-0.03	-0.06	0.11
St. Dev.	0.24	0.24	0.22	0.17
No. of pairs	21	9	7	23

f. Stability

In order to assess the utility of Nimbus 6 satellite data for the determination of air mass stability, three parameters

were computed. They are: 1) vertical lapse rate of temperature; 2) Showalter index; and 3) vertical totals index.

1) Lapse rate

In this research the computed lapse rates were normalized to °C km^{-1}. The lapse rate data were stratified into three layers: surface to 500 mb, 500 to 300 mb, and 300 to 100 mb.

Biases in the discrepancies between satellite and rawinsonde lapse rate data shown in Table 15 are within 0.3°C km^{-1} except for Area IV where the bias is -0.7°C km^{-1} in the lowest layer. This large discrepancy is caused by errors in the satellite data near the ground over the mountains. The standard deviations for each layer and area also are listed in Table 15. The smallest standard deviation occurred in the middle layer of each area with the lowest value over water (Area II). These results also can be seen from the cumulative frequency distributions shown in Figs. 32 through 35. The close agreement between satellite and rawinsonde data reflected in Table 15 and Figs. 32 through 35 attests to the high quality of the satellite temperature data.

Table 15. Means and standard deviations of discrepancies (°C km^{-1}) between Nimbus 6 satellite and weighted rawinsonde lapse rate data stratified into three layers: (A) surface to 500 mb; (B) 500 to 300 mb; and (C) 300 to 100 mb.

	Area I			Area II			Area III			Area IV		
	A	B	C	A	B	C	A	B	C	A	B	C
Mean	-0.1	0.0	-0.3	-0.1	-0.1	-0.0	0.1	-0.1	-0.1	-0.7	-0.3	-0.3
St. Dev.	1.3	0.7	1.4	0.9	0.4	0.8	1.4	0.8	1.4	1.9	0.7	1.1
No. of data	168	123	119	81	53	44	54	42	42	137	138	134

2) Showalter Index

The procedure for the computation of the Showalter Index was presented in the section on methods of data analysis. Showalter

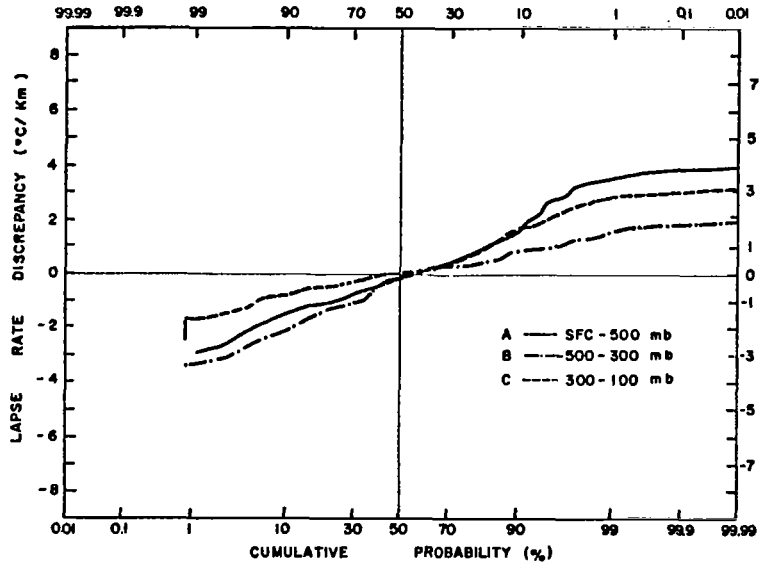

Fig. 32. Cumulative frequency distributions of discrepancies in the lapse rate of temperature within the layers surface to 500 mb, 500 to 300 mb, and 300 to 100 mb for Area I (central United States).

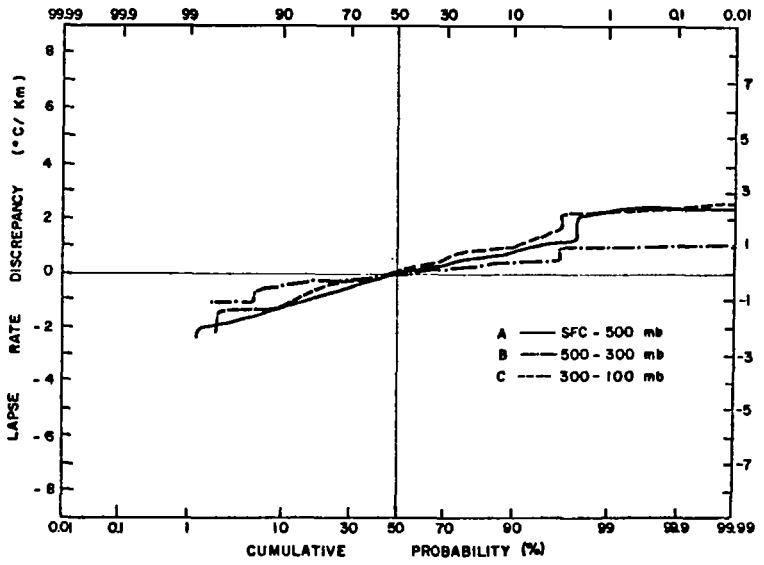

Fig. 33. Cumulative frequency distributions of discrepancies in the lapse rate of temperature within the layers surface to 500 mb, 500 to 300 mb, and 300 to 100 mb for Area II (Caribbean).

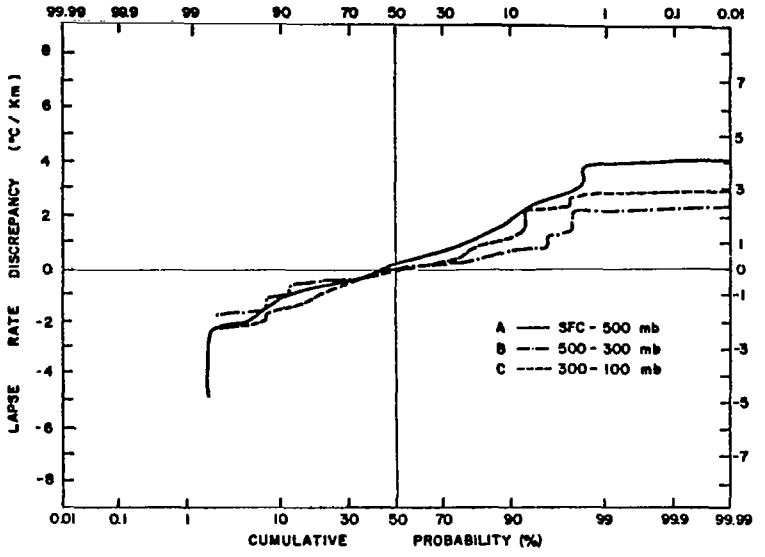

Fig. 34. Cumulative frequency distributions of discrepancies in the lapse rate of temperature within the layers surface to 500 mb, 500 to 300 mb, and 300 to 100 mb for Area III (Canada).

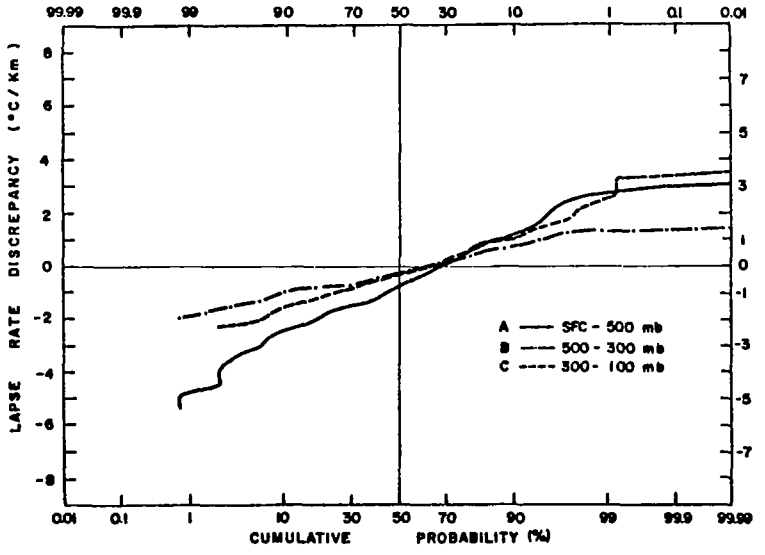

Fig. 35. Cumulative frequency distributions of discrepancies in the lapse rate of temperature within the layers surface to 500 mb, 500 to 300 mb, and 300 to 100 mb for Area IV (western United States).

indices computed from satellite and rawinsonde data and the discrepancy for each station pair for Areas I, II, III, and IV are shown in Tables 16 through 19, respectively. While no systematic relationship was found between satellite and rawinsonde Showalter indexes, it was found that all Showalter indexes computed from satellite data were positive. This is not fully understood but may be related to the temperature and moisture structure of the areas studied, or to the inaccuracies in satellite dew-point and ambient temperatures in the lower troposphere. The missing data for Area IV resulted from the surface pressure being less than 850 mb.

3) Vertical Totals Index

Smaller percentage errors in the mean discrepancies were found for the vertical totals index than for the Showalter index. Mean discrepancies of -2.1, -1.1, 0.4, and -1.6 are shown in Tables 20 through 23 for Areas I, II, III, and IV, respectively. The vertical totals indexes obtained from satellite data differ from those obtained from rawinsonde data by less than 5%. This good agreement between satellite and rawinsonde again reflects the high quality of the satellite temperature data.

Table 16. Discrepancies in the Showalter Index derived from satellite and rawinsonde data for Area I (central United States).

STATION NO.*	SATELLITE	RAWINSONDE	DISCREPANCY
235	1.7	1.4	0.3
747	3.4	6.1	-2.7
340	1.9	1.2	0.7
433	3.8	-5.6	6.7
532	3.5	3.3	0.2
655	4.2	7.4	-3.2
229	2.1	-1.1	3.2
349	2.5	-2.4	4.9
645	3.1	10.6	-7.5
247	2.0	0.8	1.2
327	2.4	0.0	2.4
456	1.9	-2.0	3.9
553	3.6	9.5	-5.9
654	4.0	5.6	-1.6
260	1.0	0.3	0.7
311	2.1	0.1	2.0
353	1.0	-2.4	3.4
429	3.0	0.0	3.0
451	1.2	-0.3	1.5
562	3.5	9.6	-6.1
734	2.1	3.5	-1.4
MEAN			0.3

* Station names are given in Appendix A.

Table 17. Same as Table 16, but for Area II (Caribbean).

STATION NO.	SATELLITE	RAWINSONDE	DISCREPANCY
201	1.7	-1.1	2.8
202	2.6	0.8	1.8
210	3.7	-0.8	4.5
644	1.9	0.6	1.3
367	3.8	-1.4	5.2
397	4.2	0.6	3.6
501	3.9	6.1	-2.2
806	0.7	2.7	-2.0
001	2.6	5.2	-2.6
MEAN			1.4

Table 18. Same as Table 16, but for Area III (Canada).

STATION NO.	SATELLITE	RAWINSONDE	DISCREPANCY
768	3.9	3.1	0.8
836	5.0	9.1	-4.1
848	6.1	5.6	0.5
867	5.3	4.3	1.0
913	2.6	1.5	1.1
934	8.5	9.3	-0.8
119	8.5	2.0	6.5
MEAN			0.7

Table 19. Same as Table 16, but for Area IV (western United States).

STATION NO.	SATELLITE	RAWINSONDE	DISCREPANCY
265	2.7	0.9	1.8
274	1.9	0.9	1.0
290	5.1	8.6	-3.5
363	1.3	0.0	1.3
365	-	-	-
374	-	0.1	-
385	5.2	7.2	-2.0
393	8.2	20.1	-11.9
451	2.3	-1.1	3.4
469	-	-	-
476	-	4.9	-
486	-	-	-
562	3.2	8.0	-4.8
572	-	8.7	-
576	-	-	-
654	6.6	8.2	-1.6
655	6.8	7.6	-0.8
662	6.4	10.6	-4.2
681	-	9.7	-
764	6.7	11.6	-4.9
768	7.2	5.5	1.7
775	8.1	6.8	1.3
785	6.2	7.9	-1.7
MEAN			-1.1

Table 20. Discrepancies in the Vertical Totals Index derived from satellite and rawinsonde data for Area I (central United States).

STATION NO.	SATELLITE	RAWINSONDE	DISCREPANCY
235	23.4	28.0	-4.6
747	23.3	22.5	0.8
340	23.9	24.7	-0.8
433	23.5	27.6	-4.1
532	24.1	25.2	-1.1
655	25.4	22.7	2.7
229	24.3	28.2	-3.9
349	23.0	27.7	-4.7
645	25.6	27.8	-2.2
247	22.9	26.2	-3.3
327	24.2	25.9	-1.7
456	23.7	25.1	-1.4
553	25.0	25.8	-0.8
654	26.2	26.5	-0.3
260	22.7	27.2	-4.5
311	23.9	28.5	-4.6
353	24.3	29.1	-4.8
429	24.0	24.6	-0.6
451	25.3	28.0	-2.7
562	26.6	26.2	0.4
734	23.1	24.8	-1.7
MEAN			-2.1

Table 21. Same as Table 20, but for Area II (Caribbean).

STATION NO.	SATELLITE	RAWINSONDE	DISCREPANCY
201	24.5	25.5	-1.0
202	23.8	25.1	-1.3
210	24.0	25.4	-1.4
644	24.5	25.6	-1.1
367	23.1	23.8	-0.7
397	23.2	23.3	-0.1
501	23.2	25.0	-1.8
806	23.5	24.8	-1.3
001	23.1	24.0	-0.9
MEAN			-1.1

Table 22. Same as Table 20, but for Area III (Canada).

STATION NO.	SATELLITE	RAWINSONDE	DISCREPANCY
768	23.8	27.8	-4.0
836	25.8	26.1	-0.3
848	24.8	21.7	3.1
867	24.7	23.4	1.3
913	23.2	20.3	2.9
934	25.3	21.4	3.9
119	24.3	28.4	-4.1
MEAN			0.4

Table 23. Same as Table 20, but for Area IV (western United States).

STATION NO.	SATELLITE	RAWINSONDE	DISCREPANCY
265	22.7	26.5	-3.8
274	25.1	32.9	-8.7
290	25.5	31.6	-6.0
363	24.0	28.2	-4.2
365	-	-	-
374	-	30.0	-
385	26.3	31.4	-5.1
393	26.6	26.4	0.3
451	24.6	32.0	-7.4
469	-	-	-
476	-	33.3	-
486	24.4	-	-
562	23.0	30.0	-7.0
572	-	28.2	-
576	24.0	-	-
654	24.9	23.6	1.3
655	24.8	21.9	2.9
662	24.4	26.4	1.9
681	-	26.0	-
764	23.7	19.1	4.6
768	23.1	24.4	-1.2
775	22.8	26.8	-4.0
785	23.7	24.7	-1.0
MEAN			-1.6

7. SUMMARY AND CONCLUSIONS

a. Summary

An analysis was conducted of satellite and rawinsonde sounding data and parameters derived therefrom for four geographical areas including the central United States, Caribbean, Canada, and western United States. Comparisons were made by using discrepancies between satellite and weighted (linearly interpolated) rawinsonde data for temperature, dew-point temperature, mixing ratio, precipitable water, thickness, lapse rate of temperature, and stability indexes. Mean and standard deviations of discrepancies of temperature, dew point, and thickness were computed. Cumulative frequency distributions of discrepancy data stratified into layers for temperature, dew-point temperature, thickness, mixing ratio, and lapse rate of temperature were presented. Precipitable water and Showalter and vertical total indexes computed from satellite and weighted rawinsonde data also were compared.

b. Conclusions

The following conclusions were reached from the results of this research:

(1) The approximate mean RMS of the discrepancies for profile pairs between satellite and weighted rawinsonde data for seven parameters are the following:

(a) Temperature: 2 C

(b) Dew-point temperature: 7.5 C

(c) Layer thickness: 7 m km^{-1}

(d) Mixing ratio: 1.34 g kg^{-1}

(e) Precipitable water: 0.23 cm

(f) Lapse rate of temperature: 1.1 C km^{-1}

(g) All Showalter indexes derived from satellite data are positive, and the vertical totals index is within 5% of and smaller than those computed from rawinsonde data.

(2) Good agreement between satellite and rawinsonde temperature data was found, although satellite moisture data are highly

questionable.

(3) The poorest agreement between satellite and rawinsonde temperature or temperature-derived parameters was found either near the tropopause region or near the ground. Average satellite temperature is higher in the tropopause region and lower near the ground than the rawinsonde temperature. The best agreement between the temperatures was found in the middle troposphere. The largest disagreement between satellite and rawinsonde dew-point temperatures was found in the layer between 500 and 300 mb.

(4) Results for the four geographical areas studied show that the best agreement between satellite and rawinsonde temperatures and parameters derived from temperature is found over water (Caribbean) and the poorest agreement was found over the mountains (western United States).

(5) In addition to instrument errors of the satellite sensors and rawinsonde observations, the discrepancies between satellite and rawinsonde data may be attributed to the following:

(a) The distance between satellite and rawinsonde station pairs;

(b) The smoothing of the satellite temperature profile due to the data processing method;

(c) Moisture effects on the satellite sensors; and

(d) The type of underlying surface; and

(e) Interpolation of the rawinsonde data.

REFERENCES

Hanel, R., and B. J. Conrath, 1969: Interferometer experiment on Nimbus 3: Preliminary Results. Science, 165, 1258-1260.

Hillger, D. W., and T. H. Von der Haar, 1977: Deriving mesoscale temperature and moisture fields from satellite radiance measurements over the United States. J. Appl. Meteor., 16, 715-726.

Horn, L. H., R. A. Petersen, and T. M. Whittaker, 1975: Intercomparisons of data derived from Nimbus 5 satellite soundings, radiosonde observations and initialized LFM model fields. Meteorological Applications of Satellite Indirect Soundings, Project Report, NOAA Grant 04-4-158-2, Dept. Meteor., University of Wisconsin, Madison. 35-70.

Miller, R. C., 1967: Notes on analysis and severe-storm forecasting procedures of the Military Weather Warning Center. AWS Tech. Report 200, 94 pp.

Moyer, V., J. R. Scoggins, N. Chou, and G. S. Wilson, 1978: Atmospheric Structure Deduced from Routine Nimbus 6 Satellite Data. Mon. Wea. Rev., 106, 1340-1352.

Shenk, W. E., and V. V. Salomonson, 1970: Visible and infrared imagery from meteorological satellites. Appl. Opt., 9, 1747-1760.

Showalter, A. K., 1953: A stability index for thunderstorm forecasting. Bull. Amer. Meteor. Soc., 34, 250-252.

Smith, W. L., H. M. Woolf, C. M. Hayden, and W. C. Shen, 1975: Nimbus 5 sounder data processing system; Part II: Results. NOAA Technical Memorandum NESS 57, National Environmental Satellite Service, National Oceanic and Atmospheric Administration, Washington, D. C.

_____, P. G. Abel, H. M. Woolf, A. W. McCulloch, and B. J. Johnson, 1975: The high resolution infrared radiation sounder (HIRS) experiment. The Nimbus-6 User's Guide, NASA Goddard Space Flight Center, Greenbelt, Md., 37-58.

Staelin, D. H., F. T. Barath, J. C. Blinn III, and E. J. Johnston, 1972: The Nimbus-E microwave spectrometer (NEMS) experiment. The Nimbus-5 User's Guide, NASA Goddard Space Flight Center, Greenbelt, Md., 141-157.

_____, A. H. Barrett, and J. W. Waters, 1973: Microwave Spectrometer on the Nimbus 5 satellite: Meteorological and

Geophysical data. Science, 182, 1339.

_____, _____, P. W. Rosenkranz, F. T. Barath, E. J. Johnson, J. W. Waters, and A. Wouters, 1975: The scanning microwave spectrometer (SCAMS) experiment. The Nimbus-6 User's Guide, NASA Goddard Space Flight Center, Greenbelt, Md., 59-86.

Wark, D. Q., and D. T. Hilleary, 1969: Atmospheric temperature: Successful test of remote probing. Science, 165, 1256-1258.

Waters, J. W., K. F. Kunzi, R. L. Pettyjohn, R. K. L. Poon, and D. H. Staelin, 1975: Remote sensing of atmospheric temperature profiles with the Nimbus 5 microwave spectrometer. J. Atmos. Sci., 32, 1953-1969.

Weinreb, M. P., 1977: Sensitivity of satellite retrievals of temperature to errors in estimates of tropospheric water vapor. J. Appl. Meteor., 16, 605-613.

Wilcox, R. W., and F. Sanders, 1976: Comparison of layer thickness as observed by Nimbus E microwave spectrometer and by radiosonde. J. Appl. Meteor., 15, 956-961.

APPENDIX A

Rawinsonde stations used in each area.

Area I - Central United States

Station	Identifier	Location
72229	CKL	Centerville, Alabama
72235	JAN	Jackson, Mississippi
72247	GGG	Longview, Texas
72260	SEP	Stephenville, Texas
72311	AHN	Athens, Georgia
72327	BNA	Nashville, Tennessee
72340	LIT	Little Rock, Arkansas
72349	UMN	Monette, Missouri
72353	OKC	Oklahoma City, Oklahoma
72429	DAY	Dayton, Ohio
72433	SLO	Salem, Illinois
72451	DDC	Dodge City, Kansas
72456	TOP	Topeka, Kansas
72532	PIA	Peoria, Illinois
72553	OMA	Omaha, Nebraska
72562	LBF	North Platte, Nebraska
72645	GRB	Green Bay, Wisconsin
72654	HON	Huron, South Dakota
72655	STC	St. Cloud, Minnesota
72734	SSM	Sault Sainte Marie, Michigan
72747	INL	International Falls, Minnesota

Area II - Caribbean

Station	Identifier	Location
72201	EYW	Key West, Florida
72202	MIA	Miami, Florida
72210	FMY	Fort Myers, Florida
76644	MID	Merida, Mexico
78367	MUGM	Guantanamo, Cuba
78397	MKJP	Kingston, Jamaica
78501	KSWA	Swan Island, Swan Island
78806	MBHO	Howard, Panama
80001	MCSP	San Andres, Colombia

APPENDIX A (Continued)

Area III - Canada

Station	Identifier	Location
72768	GGW	Glasgow, Montana
72836	YMO	Moosonee, Canada
72848	YTL	Trout Lake, Canada
72867	YQD	The Pas, Canada
72913	YYQ	Churchill, Canada
72934	YSM	Fort Smith, Canada
74119		Edmonton, Canada

Area IV - Western United States

Station	Identifier	Location
72265	MAF	Midland, Texas
72274	TUS	Tucson, Arizona
72290	SAN	San Diego, California
72363	AMA	Amarillo, Texas
72365	ABQ	Kirtland, New Mexico
72374	INW	Winslow, Arizona
72385	UCC	Yucca Flats, Nevada
72393	VBG	Vandenburg, California
72451	DDC	Dodge City, Kansas
72469	DEN	Denver, Colorado
72476	GJT	Grand Junction, Colorado
72486	ELY	Ely Yelland, Nevada
72562	LBF	North Platte, Nebraska
72572	SLC	Salt Lake City, Utah
72576	LND	Lander, Wyoming
72654	HON	Huron, South Dakota
72655	STC	St. Cloud, Minnesota
72662	RAP	Rapid City, South Dakota
72681	BOI	Boise, Idaho
72764	BIS	Bismarck, North Dakota
72768	GGW	Glasgow, Montana
72775	GIF	Great Falls, Montana
72785	GEG	Spokane, Washington

APPENDIX B

Distance (km) between each pair of rawinsonde and satellite soundings for each area.

Area I - Central United States

Station number	Distance
229	86.4
235	86.4
247	104.9
260	123.4
311	185.2
327	74.1
340	123.4
349	172.8
353	216.0
429	246.9
433	61.7
451	24.7
456	104.9
532	148.1
553	117.3
562	142.0
645	142.0
654	74.1
655	129.6
734	86.4
747	123.4

Area II - Caribbean

Station number	Distance
201	117.3
202	123.4
210	123.4
644	135.8
367	432.0
397	160.5
501	234.5
806	160.5
001	111.1

APPENDIX B (Continued)

Area III - Canada

Station number	Distance
768	246.9
836	407.4
848	234.5
867	98.7
913	308.6
934	246.9
119	222.2

Area IV - Western United States

Station number	Distance
265	209.8
274	24.7
290	148.1
363	246.9
365	111.1
374	104.9
385	185.2
393	117.3
451	179.0
469	185.2
476	234.5
486	104.9
562	160.5
572	86.4
576	308.6
654	86.4
655	246.9
662	49.4
681	185.2
764	61.7
768	123.4
775	74.1
785	111.1

1. REPORT NO.	2. GOVERNMENT ACCESSION NO.	3. RECIPIENT'S CATALOG NO.
NASA RP-1073		

4. TITLE AND SUBTITLE	5. REPORT DATE
Comparisons Between Nimbus 6 Satellite and Rawinsonde Soundings for Several Geographical Areas	January 1981
	6. PERFORMING ORGANIZATION CODE
7. AUTHOR(S)	8. PERFORMING ORGANIZATION REPORT #
Nine-Min Cheng and James R. Scoggins	
9. PERFORMING ORGANIZATION NAME AND ADDRESS	10. WORK UNIT NO.
Department of Meteorology Texas A&M University College Station, Texas 77843	M-330
	11. CONTRACT OR GRANT NO.
	13. TYPE OF REPORT & PERIOD COVERED
12. SPONSORING AGENCY NAME AND ADDRESS	Reference Publication
U.S. Army Research Office Research Triangle Park, North Carolina	14. SPONSORING AGENCY CODE

15. SUPPLEMENTARY NOTES

The U. S. Army Research Office has granted permission for NASA to publish these data for use in studies using space technology for weather-related programs.

16. ABSTRACT

Discrepancies between Nimbus-6 satellite and weighted rawinsonde data on 25 August 1975 and 3 September 1975 are examined over four geographical areas. Good agreement between satellite and weighted (linearly interpolated) rawinsonde temperature and temperature-derived parameters was found in most instances, with the poorest agreement either near the tropopause region or near the ground. However, satellite moisture data are highly questionable. The smallest discrepancy between satellite and weighted mean rawinsonde temperature and parameters derived from temperature was found over water, and the largest discrepancy was found over mountains. Cumulative frequency distributions show that discrepancies between satellite and rawinsonde data can be represented by a normal distribution except for dew-point temperature.

17. KEY WORDS	18. DISTRIBUTION STATEMENT
Meteorological satellite data Satellite-derived soundings Satellite-derived winds	Unclassified - Unlimited Subject Category 47

19. SECURITY CLASSIF. (of this report)	20. SECURITY CLASSIF. (of this page)	21. NO. OF PAGES	22. PRICE
Unclassified	Unclassified	75	A04

For sale by National Technical Information Service, Springfield, Virginia 22161

NASA-Langley, 1981